Design of Binary and Ternary Nitrate Salt Mixtures for Energy Storage and Heat Transfer in Solar Thermal Systems

A Dissertation submitted
in partial fulfilment of the requirements
for the award of degree of

Master of Engineering

in

Thermal Engineering

by

Abhishek Upadhyay

Registration No.: 801483002

Under the Supervision of

Dr. MADHUP KUMAR MITTAL
(Assistant Professor)

DEPARTMENT OF MECHANICAL ENGINEERING

THAPAR UNIVERSITY, PATIALA

July, 2016

CERTIFICATE

I hereby declare that the thesis entitled "**Design of binary and ternary nitrate salt mixtures for energy storage and heat transfer in solar thermal systems**" is an authentic record of my work carried out as requirements for the award of the degree of **Master of Engineering** in **Thermal Engineering** at **Thapar University, Patiala**, Punjab under the supervision of **Dr. Madhup Kumar Mittal**, Assistant Professor, Mechanical Department, Thapar University, Patiala during July, 2014 to July, 2016. No part of the matter embodied in this report has been submitted to any other university or institute for the award of any degree.

Date: 07/07/2016

Abhishek Upadhyay

It is certified that the above statement made by the student is correct to the best of my knowledge and belief.

Dr. Madhup Kumar Mittal
Mechanical Engineering Department
Thapar University, Patiala – 147004

Countersigned by

Head, Mechanical Engineering Department
Thapar University, Patiala – 147004

Dean of Academic Affairs
Thapar University, Patiala - 147004

Dedication

I dedicate this thesis to my beloved father Sanjay Kumar Sharma and my mother Dipti Sharma, who are an ever supporting and encouraging with their great patience. I also dedicate this to my sister Jagritee Upadhyay, who is as an impression for me and to all my dearest friends.

Acknowledgements

First of all, I would like to thanks to my supervisor Dr. Madhup Kumar Mittal, Assistant Professor, Thapar University, Patiala for their worthy guidance, continuous encouragement and having high patience to listen to all my queries and suggest accordingly. The faith of Dr. Madhup Kumar Mittal in me always compelled me to work hard, apart from thesis his attitude towards life, work and valuable words taught me many things. The hard work and practical knowledge of Mr. Gurpindar Dhindsa, Thapar University stood as an inspiration for me. A special thanks to Mr. Ravindra Kaushal, Thapar University for their assistance to make my avail with the material required for my project work.

I would like to acknowledge all the members of Physics Department, Thapar University for helping me to carry out experimental work.

I appreciate the facilities provided by Thapar University to carry out my studies and gain practical knowledge. I gratefully acknowledge Institute Instrumentation Centre, Indian Institute of Technology Roorkee for providing the TGA and DSC experimental facility.

A special debt of gratitude is owed to the authors whose work I have consulted and quoted in this work.

Last but not least I am always grateful to my family and friends for their unconditional support, encouragement and best wishes, without which I have not come this far.

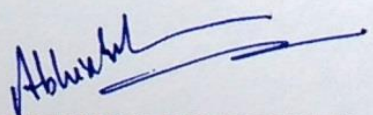

ABHISHEK UPADHYAY

Abstract

The objective of the present study is to obtain molten salt having higher thermal stability, reduced cost and relatively lower melting point as compared to previously available molten salts. A very large range of molten blends of alkali nitrates are inspected by experimental approach. Since the determination of eutectic concentration, melting point and phase diagram from experimental methods are usually costly and time consuming; therefore it is of interest to predict the same by using some numerical method. In this work, the numerical method based on regular solution theory is used to predict eutectic concentration and melting point of the binary and ternary systems consisting of $NaNO_3$, KNO_3 and $LiNO_3$ salts. The melting points of binary and ternary systems are also determined experimentally using Differential Scanning Calorimeter (DSC) and then they are compared with those predicted by the numerical method. Thermo-Gravimetric analysis (TGA) is also used to determine thermal stability of three binary and a ternary mixtures at various temperature. The experimental values obtained from instruments are found to be in good agreement with the predicted values obtained from numerical method. The experimental results show that the ternary salt studied in this work has a melting point of 121°C. This salt mixture is thermally stable up to temperature of 534°C and can be used up to a temperature of 608°C for a short period of time. This ternary salt mixture is also cost effective due to lower concentration of lithium nitrate in the salt mixture.

Key words: Nitrate salt mixtures; eutectic composition; regular solution theory; phase diagram; solar energy.

Contents

List of Figures

List of Tables

Nomenclature

ΔG^A:	The gibbs free energy of component A (J/g)
ΔH_f^A:	Enthalpy and of fusion of component A (J/g)
ΔH_f^B:	Enthalpy and of fusion of component B (J/g)
ΔH_f^C:	Enthalpy and of fusion of component C (J/g)
ΔH_m^A:	Partial enthalpy of mixing of component A (J/g)
ΔH_m:	Enthalpy of mixing (J/g)
ΔS_f^A:	Entropy of fusion of component A (J/K)
ΔS_m^A:	Partial entropy of mixing of component A (J/K)
ΔC_{PA}:	Change in specific heat of component A during phase change (J/g)
ΔC_{PB}:	Change in specific heat of component B during phase change (J/gK)
ΔC_{PC}:	Change in specific heat of component B during phase change (J/gK)
T_M^A:	Melting point of component A (°C)
T_M^B:	Melting point of component B (°C)
T_M^C:	Melting point of component C (°C)
T:	Temperature at particular mole fraction (°C)
x_A:	Mole fraction of component A (mol.)
x_A^l:	Mole fraction of liquidus part of component A(mol.)
x_A^s:	Mole fraction of solidus part of component A (mol.)
x_B^l:	Mole fraction of liquidus part of component B (mol.)
x_B^s:	Mole fraction of solidus part of component B (mol.)
x_C^l:	Mole fraction of liquidus part of component C (mol.)
x_C^s:	Mole fraction of solidus part of component C (mol.)

a, b, and c:	Empirical coefficients

Acronyms

DSC:	Differential Scanning Calorimetry
TGA:	Thermogravimetric Analysis
TES:	Thermal Energy Storage
HTF:	Heat Transfer Fluid
DTA:	Differential Thermal Analysis
HCE:	Heat Collector Element

Chapter 1

Introduction

1.1 Introduction

The gradually rising price of fossil fuel and concerning shrinkage of reservoirs, there is an extensive demand for green and affordable renewable source of energy to fulfil the rising energy demands of the world. The sun is largest source of green energy and has an adequate potential to fulfil the energy demands for the present as well as forthcoming generation. In spite of this, the electricity produced from the solar energy is only a fraction of the total world's power consumption. Over the last few decades, a lot of research has been carried out to harvest the solar energy. The main problem faced by solar energy based thermal systems is the intermittent supply of solar energy during cloudy days and night. The problem of intermittent supply of solar energy can be overcome by using thermal energy storage material. In concentrating solar power plants thermal energy storage materials (TES) are utilised to provide heat energy in absence of beam radiation [1].

Out of various types of TES used in solar thermal systems, molten salts are studied widely due to various advantages such as high working temperature (>550°C,) good physical and thermal properties at elevated temperature, low corrosiveness, low vapour pressure and high heat capacity. The current technology generally uses high-temperature mineral and synthetic oils which are flammable and can be used only up to a temperature of 393°C. Due to low value of maximum usable temperature of mineral and synthetic oils, the Rankine efficiency of the power block steam turbine is limited to 37.6%. However, the maximum fluid output temperature with molten salts can be achieved up to 500-550°C that helps to achieve the Rankine efficiency of steam power block up to 40%, thus reducing energy cost to 2 cents/KWh [2]. The different types of molten salts that can be used as an energy storage and heat transfer in solar power plants are the chlorides, carbonates, nitrates, and fluorides. The fluoride molten salts are used in nuclear reactor and space solar power system due to their high storage capacity, but they have disadvantages like high cost, toxicity, and material compatibility [3]. The chlorides may be preferred due to their high heat of fusion and low cost, but their high corrosiveness makes them less attractive [4]. The carbonates are attractive for high temperature latent heat storage applications such as solar power towers, but they are

less attractive in terms of ease of decomposition and high viscosity [5]. The most reliable eutectics are of nitrate and nitrite salts because of advantages such as low chemical reactivity, low cost, less corrosiveness [6]. Therefore in solar thermal power plant, eutectics of nitrate and nitrite salts are considered to be reliable as thermal energy storage material and heat transfer fluid.

There is wide range of commercially available mixtures of nitrates or nitrites salts and few of them have been used in solar power plant. The binary salt mixture popularly known as solar salt (40% wt KNO_3 and 60% $NaNO_3$) is used at Solar 2, a heliostat collector project in California [7] and this salt also provides indirect viable option of thermal energy storage for Andasol Plant Spain [8]. This binary mixture has higher dissociation temperature of 600°C and lower cost as compared with synthetic oil. The Hitech salt which is a ternary mixture has been used for decades in heat treating industry. This salt has an advantage of low melting point but starts dissociating at a temperature of 454°C, and may be used for a short period of time up to temperature of 538°C [8]. Few research studies have been reported on more complex salt mixture such as, Hitec XL which is eutectic mixture of $NaNO_3$, $Ca(NO_3)_2$, KNO_3 salts [9] and it has melting temperature of 133°C. The quaternary nitrate mixture of salts Lithium, Potassium, Calcium and Sodium cations have melting point of 100°C [10] . A blend of anion Nitrite/Nitrate and cations Potassium, Sodium and Lithium start meting below 80°C [11]. A pentane mixture of Nitrate of Caesium, Calcium, Lithium, Sodium and Potassium has melting point as low as 65°C [12]. Since millions of kilograms of salt is required as HTF in solar power plant for energy storage, therefore the drawback of the above discussed ternary, quaternary and pentane salt mixtures is that they are expensive due to presence of high concentration of Caesium and Lithium Nitrate in them. Moreover the presence of Calcium Nitrate increases viscosity and density of mixture of salts. Therefore, it is important to develop a salt mixture that has low cost along with the favourable physical and thermal properties.

Experimental methods can be used to determine thermodynamic properties and phase transition of mixture of higher order salts. However, the experimentation methods are time consuming and expensive, therefore it is of interest to be able to predict the thermodynamic property and phase diagram of higher order salts using the numerical method along with the available data of lower order salts.

In this work, the three binary and one ternary salt mixture consisting of $NaNO_3$, KNO_3 and $LiNO_3$ salts are studied theoretically and experimentally. First of all, the eutectic concentration and melting temperature of the salt mixtures is determined by using numerical method based on regular solution theory. Then thermal stability and melting point of these salt mixtures at eutectic concentration are determined using Thermo-Gravimetric Analysis (TGA) and Deferential Scanning Calorimetry (DSC) instruments. The mathematical model has been used to develop phase diagrams for all the three binary salt mixtures. The theoretical phase diagrams are also compared with the experimental data available in the open literature.

1.2 Objectives

In view of the above mentioned research gaps, the following specific objectives are undertaken:

i. To develop a low melting point molten salt system for thermal energy storage in solar power plant using thermodynamic model.
ii. To test and verify melting point of thermal energy storage material.
iii. To determine the thermal stability of low melting point molten salt system.
iv. To improve the performance, stability and cost-effectiveness of new storage material.

Chapter 2

Literature Review

The literature review shows the detailed discussion about the application of molten salt mixtures used in solar thermal power plant as heat storage material and heat transfer fluid. Molten salts exhibits a great potential and a wider scope when applied in a heat transfer and energy storage related problems. Firstly, literature based on heat transfer fluids which are currently in use for solar thermal energy storage in concentrated solar power systems(CSP) and discussing the methods of determination of properties such as viscosity, thermal capacity, thermal conductivity, melting temperature, thermal stability and corrosion rate and how these properties affecting the performance of solar thermal systems are reviewed. In later part the effect of usage of $LiNO_3$ and $CsNO_3$ on the cost and performance of heat transfer fluid is highlighted in this study.

2.1 Previous Research Work

Glatzmaier G.C. et al. [1] In this research article the author discuss about the store thermal energy, sensible and latent heat storage materials. The author discuss that latent heat thermal energy storage (TES) systems using phase change materials (PCM) are useful because of their ability to charge and discharge a large amount of heat from a small mass at constant temperature during a phase transformation. Because high-melting-point PCMs have large energy densities, their use can reduce energy storage equipment and containment costs by decreasing the size of the storage unit. Using cascaded PCMs, with equally spaced melting points and with high thermal properties, the TES is significantly enhanced. However, currently there is not enough information on the thermal properties of molten salt systems at high temperatures.

Molten salt PCM candidates for cascaded PCMs were evaluated for the temperatures near 320°C, 350°C, and 380°C. These temperatures were selected to fill the 300°C to 400°C operating range typical for parabolic trough systems, that is, as one might employ in three-PCM cascaded thermal storage. Such systems require a series of PCMs with melting points spanning the range of TES. The molten salt systems considered in this study were KNO_3-KCl-KBr, NaCl – KCl - LiCl and $MgCl_2$-KCl-NaCl. Because the majority of the salts studied

were hygroscopic, a handling and mixing protocol under controlled atmosphere was employed. The mixing procedure was carefully controlled because the sample weight required for the thermal property tests is on the order of a few milligrams, so a perfectly homogenized sample is essential for accurate results. Heat capacity, latent heat, transformation temperatures, thermal stability, and viscosity were measured. Before performing these evaluations, chemical stability (corrosion) of the container materials with the molten salts was evaluated in a controlled atmosphere furnace under nitrogen gas. The materials tested were 316 stainless steel (SS316), high purity aluminium (Al1100), aluminium-manganese alloys (Al3003) and aluminium oxide (Al_2O_3). Based on the results, the best candidate for temperatures near 320°C was the molten salt KNO_3-4.5wt%KCl. For the 350°C and 380°C temperatures, the evaluated molten salts are not good candidates because of the corrosiveness and the high vapour pressure of the chlorides.

Kearney D. et al. [2] In this study the author done an evaluation to investigate the feasibility of utilizing a molten salt as the heat transfer fluid (HTF) and for thermal storage in a parabolic trough solar field to improve system performance and to reduce the levelled electricity cost. The author reported that the operating SEGS 1 plants currently use high temperature synthetic oil consisting of a eutectic mixture of biphenyl/diphenyl oxide. The scope of this investigation included examination of known critical issues, postulating solutions or possible approaches where potential problems existed, and the quantification of performance and electricity cost using preliminary cost inputs. The two leading candidates were the so-called solar salt (a binary salt consisting of 60% $NaNO_3$ and 40% KNO_3) and a salt sold commercially as HitecXL (a ternary salt consisting of 48% $Ca(NO_3)_2$, 7% $NaNO_3$, and 45% KNO_3). According to the author a 2-tank storage system and a maximum operation temperature of 450°C, the evaluation showed by the author that the levelled electricity cost can be reduced by 14.2% compared to a state-of-the-art parabolic trough plant, such as the SEGS plants in California. If higher temperatures are possible, the improvement may be as high as 17.6%. Thermocline salt storage systems offer even greater benefits.

Peng Q. et al.[8] In order to obtain molten salt with lower melting point, higher thermal stability and reduced cost relative to previously available materials, the author studied variety of molten salt mixtures of alkali nitrates are investigated experimental methods. Author also used mathematical model, since measurements are generally expensive and time-consuming, it is of interest to be able to predict melting point and the component of multi-component

systems by using the numerical methods. In this paper, the author find the eutectic point and component of a new kind of the quaternary reciprocal system (K, Na/NO_2, Cl, NO_3) are determined firstly by conformal ionic solution theory. Then thermal stability of the mixtures that show a lower melting point is measured by thermogravimetric analysis device. Experimental results obtained by the author are in the agreement between measurements and calculations are found to be very good. This kind of molten salt has a lower melting point, 140 °C. It is thermally stable at temperatures up to 500 °C, and may be used up to 550 °C for short periods. Besides, this author also find a novel molten salt that has a reduced cost relative to previous low-melting nitrate mixtures due to the elimination of caesium nitrate and lithium nitrate.

Bradshaw R. et al. [10] Multi-component molten salts have been formulated by author recently that may enhance thermal energy storage for parabolic trough solar power plants. In this paper author presents further developments regarding molten salt mixtures consisting of common alkali nitrates and either alkaline earth nitrates or alkali nitrite salts that have advantageous properties for applications as heat transfer fluids in parabolic trough systems. According to the report submitted by the author, the results for formulations of inorganic molten salt mixtures that display freeze-onset temperatures below 100°C. In addition to phase change behaviour, several properties of these molten salts that significantly affect their suitability as thermal energy storage fluids were evaluated, including chemical stability and viscosity. The nitrate-based molten salts have demonstrated chemical stability by the author in the presence of air up to 500°C. According to the report capability to operate at temperatures up to 500°C may allow an increase in maximum temperature operating capability vs. organic fluids in existing trough systems and will enable increased power cycle efficiency. Experimental measurements of viscosity were performed by author from near the freeze-onset temperature to about 200°C. Viscosities can exceed 100 cP near the freezing temperature but are 4 to 5 cP in the anticipated operating temperature range. Corrosion tests were conducted by author for several thousand hours at 500°C with stainless steels and at 350°C for carbon and chromium-molybdenum steels. Examination of the specimens demonstrated good compatibility of these materials with the molten nitrate salt mixtures. Laboratory studies were conducted by author to identify mixtures of nitrate and nitrite (NO_2) salts as additional candidates for a low-melting heat transfer fluid. Mixtures in which the cations were potassium, sodium and lithium, in various proportions, demonstrated freezing points as low as 70°C for a particular nitrate/nitrite anion composition. In this development

author has emphasized mixtures that minimize lithium content in order to reduce the cost as the lithium salt is the most expensive constituent. The results reported by author to date indicate that the viscosity of these mixtures is considerably less than nitrate-only melts, which necessarily contain calcium cations to suppress freezing to similarly low temperatures.

Vignarooban et al. [13] has described about various heat transfer fluid which are currently in use for solar thermal energy storage in concentrated solar power systems (CSP). In this research paper, they have reviews various types of heat transfer fluid (HTF) such as air, water/steam, thermal oil, molten salts and liquid metals in details with the properties like viscosity, thermal capacity, thermal conductivity, melting temperature, thermal stability and corrosion rate. Solar power tower is the current and future need of CSP systems. Because a very high temperature can be maintained in the receiver. Which leads to the generation of electricity more efficiently. In the currently solar power tower plants the temperature limit is in between 300 and 560℃. in future the temperature limit up to 800℃ can be achieved. So at that high temperature limit, molten salts with high boiling point can be used in the forthcoming solar power tower plants. Most of the molten salts are based on nitrate/nitrate. The largest accumulations of naturally occurring sodium nitrate are found in Chile and Peru. However, the annual nitrate/nitrite salts production is limited due to their reserves. Therefore, carbonate or chloride-based salts are proposed and evaluated in the most recent studies. They also have emphasized that initially in solar electric generating system 1(SEG1) solar salt $NaNO_3$(60wt%)-KNO_3(40wt%) was used as a heat transfer fluid and storage media. . It melts at 223 ℃ and remains in thermally stable liquid phase at temperatures up to 600℃. The problem of this salt was high melting point. So to lower down the melting temperature, researcher introduced another salts name Hitech, HitechXL. These salts have lower melting point (142℃,120℃ respectively) but have lower thermal stability temperature ~500℃. Corrosion rates of different piping material such as stainless steel and nickel base alloys in different heat transfer fluid are also discussed in terms of corrosion rate.

Zhai et al. [14] in this research paper, they have performed experimental analysis on molten two salts. They have optimized the various parameter of solar two molten salt by adding three different additives (Additive-A, Additive-B, Additive-c) in three different concentrations (2%,5% and 10%) such as melting point and specific heat capacity. In the results they found that the additive -A can optimize the melting point and heat of fusion of molten slats (melting point-205.6℃, heat of fusion-113.23J/g). Additive-B and additive-c have good effect only in

melting point but heat of fusion very much reduced. so solar two salt with 10% additive A has improved the thermal performance of heat transfer and storage of the thermal material.

Fernández et al. [15] in this research paper they have suggested a material alumina forming stainless steel (C-4, Fe-25, Ni-14, Cr-3.5, Al-2.5, Nb-2 wt. % base) as a candidate material for the solar power plant heat exchanger and pipes. They have studied the Corrosion behaviour of C-4, relative to 304 stainless steel and T22 steel by gravimetric analysis and electrochemical impedance spectroscopy. Experimental C-4 steel showed excellent behaviour in the NaNO_3:KNO_3 salt mixture (60:40 ratio) compared to the AISI 304 and T22 steels. Corrosion tests performed and the characterization of the surface carried out after them. Virtually no attack occurred up to 2000 hr. of immersion of the steel in the molten salt, based on gravimetric analysis. This suggests the formation of a highly protective layer, consistent with Al-Cr rich oxide developed on the C-4 steel surface. The levels of chloride, sulphates, and nitrites in the molten salt after the corrosion tests suggested a limited role on corrosion of the C-4 steel maintaining similar values to the initial contents. The use of this material in pipes and heat exchangers in contact with salt molten fluid employed as energy storage in parabolic trough solar plants has been validated. The application of the C-4 steel in solar power plants will be studied in future studies, where the temperature reaches 565℃

Fernandez et al. [16] In this research paper they have studied the effect of addition of LiNO3/Ca(NO3)2 to solar salt. They made three ternary salts first 48% Ca(NO_3)$_2$ + 7% NaNO_3 + 45% KNO_3, second 20% LiNO_3 + 52% KNO_3 + 28% NaNO_3, third 30% LiNO_3 + 60% KNO_3 + 10% Ca(NO_3)$_2$ and perform thermal analysis by differential scanning calorimetry (DSC) and thermogravimetric analysis(TGA) to obtained the phase transition, melting point, heat capacity and thermal stability of the ternary mixture. In their study they found that the following results shown in the table below. Form the table they analysed that the addition of LiNO_3 increases the thermal capacity and addition of Ca(NO_3)$_2$ reduces the melting point and reduces the cost of the mixture. They proposed this mixture 30% LiNO3 + 60% KNO_3 + 10% Ca(NO_3)$_2$ for allowing direct use as storage material in parabolic- trough solar power plane.

Oliver et al.[17] Has investigated the thermal stability of Li-Na-K carbonate salt in a different environment of argon, air and CO_2. The thermal stability of a molten Li-Na-K carbonate salt was studied up to a temperature of 1000 ℃. The salt (Li_2CO_3–Na_2CO_3-

K_2CO_3) investigated was eutectic in the proportions (32.1–33.4–34.5 wt.%). The thermal analysis of the ternary salt was done by simultaneous differential scanning calorimetry (DSC) and thermogravimetric–mass spectrometric (TG–MS) analysis in gas atmospheres of argon, air, and CO2. After investigation It was found that, under a blanket gas atmosphere of

Table 2.1 Thermal properties of new molten salts developed. Fernandez et al[16].

Molten salt	Melting point (℃)	Thermal stability (℃)	Heat capacity j/g (℃)
60% NaNO_3 + 40% KNO_3	221.04	588	1.498
48% Ca(NO_3)$_2$ + 7% NaNO_3 + 45% KNO_3	130.61	524.34	1.272
20% LiNO_3 + 52% KNO_3 + 28% NaNO_3	130.15	600.05	1.091
30% LiNO_3 + 60% KNO_3 + 10% Ca(NO_3)$_2$	132.15	567.18	1.395

CO_2 the Li-Na-K carbonate salt is stable up to at least 1000 C. In an inert atmosphere of argon, the salt evolves gaseous CO_2 soon after melting and begins to decompose at between 710℃ and 715℃. Under a blanket atmosphere of air, the CO_2 evolution from the salt is observed to commence at 530℃, the onset of decomposition detected by DSC analysis at 601℃ and the rapid rate of weight loss determined by TG analysis at 673℃. The melting point of Li-Na-K salt was in the range 400-405℃. They found very less change in the melting point of the Li-Na-K salt.

Kuravi et al. [18] In this research paper they have describe the development of latent heat thermal energy storage system. Latent heat storage systems have higher energy density compare to sensible heat storage systems. But most of the phase change materials have low thermal conductivity so to improve the thermal conductivity they have coated the porous pellet with encapsulation material (SiO_2) using low cost techniques. They have used sodium nitrate (NaNO_3) as a phase change material and have used two techniques (wet granulation through agglomeration, table press method) for fabrication. Initially porous pellet with certain void space are fabricated. Due to void spaces, PCM impose less stress on the shell during

melting. They have estimated that this technique has the potential to reduce the cost of thermal energy storage system to less than $15/kWh.

Zhao et al.[19] in this research paper have a reported a novel ternary salt mixture with 50–80 wt.% KNO_3, 0–25 wt. % $LiNO_3$ and 10–45 wt% $Ca(NO_3)_2$with a low melting temperature below 100℃ and high temperature durability. The found those, in the presence of air atmosphere, this salt remain stable at approximately 450℃, which is more than the thermal stability limit of existing organic fluid. Therefore, leads to a higher thermal efficiency (Rankine Cycle efficiency) for those existing through systems. They thermal properties are measured by Simultaneous Thermal Analyzer (STA-1500). The viscosity of the samples was measured by Malvern Kinexus rheometer and found the viscosity less than 10 cP. Which directly indicated that the flow resistance will be reduced if they are used as the heat transfer fluids in a solar thermal system, compared to HitecXL or synthetic oil. the desirable thermal and transport properties of these novel nitrate salt mixtures, including low melting point, high temperature, chemical stability, low viscosity, Corrosion rate etc. make them more suitable to use as a heat transfer fluids(HTFs) than synthetic oils which is very costly and still using in solar systems.

Wang T. et al. [20] In this the author designed a novel eutectic composition in the LiF–Na_2CO_3–K_2CO_3 ternary system was predicted in this study using thermodynamic modeling based on Gibbs energy of fusion and designed for thermal energy storage or metal heat treatment. The Differential Calorimetry Scanning (DSC) technique was used by the author to experimentally measure the melting point of the eutectic composition in the ternary system which was determined to be 694.40 K. Heat capacity of the eutectic composition of the ternary system was also measured by author using DSC from solid to liquid state and the results were plotted by author as function of temperature. The upper temperature limit for thermal stability of the eutectic mixture was determined by author in different atmospheres using the Thermogravimetric Analyser (TGA). The author reported high upper temperature limit for thermal stability and ensures the large working temperature range of the LiF–Na_2CO_3–K_2CO_3 ternary system. Thermal conductivity of the ternary system was also studied by author using a simplified inverse method. The relatively high thermal conductivity indicates its high efficiency of energy storage. Based on the measured thermodynamic properties, physical properties and its high energy storage density, by author this ternary system can be used as heat transfer fluid for thermal energy storage application.

Coscia K. et al. [21] In this paper author reported that**,** current heat transfer fluids for concentrated solar power applications are limited by their high temperature stability. Other fluids that are capable of operating at high temperatures have very high melting points. The present work the author is aimed at characterizing potential solar heat transfer fluid candidates that are likely to be thermally stable (up to 500 °C) with a lower melting point (100 °C). Binary and ternary mixtures of nitrates have the potential for being such heat transfer fluids. To characterize such eutectic media, both experimental measurements and analytical methods resulting in phase diagrams and other properties of the fluids are essential. Solidus and liquidus data have been determined using a differential scanning calorimeter over the range the compositions for each salt system and mathematical models have been derived using Gibbs Energy minimization. The Gibbs models presented in this paper the author sufficiently fit the experimental results as well as providing accurate predictions of the eutectic compositions and temperatures for each system. The methods developed by the author here are expected to have broader implications in the identification of optimizing new heat transfer fluids for a wide range of applications, including solar thermal power systems.

Kramer C.M. et al. [22] The binary phase diagram of $NaNO_3$ and KNO_3 was studied by the author using differential scanning calorimetry (DSC). The data more precisely defined by the author solidus and liquidus of an earlier phase diagram for this system. This phase diagram was modelled by author using regular solution theory. By fitting the model to the experimental data the regular solution parameters and the heat of mixing for the solid solution of $NaNO_3$ and KNO_3 were estimated by the author.

Zhang X. et al. [23] The binary phase diagram of $LiNO_3$–KNO_3 is studied by the author by means of differential scanning calorimeter (DSC). The convincing evidence for the identification of new phase has been presented by the author. The phase diagram reported by the author indicates an intermediate compound $KLi(NO_3)_2$, which melts congruently at 428 K. The coordinates of two eutectic points reported by the author are 420 K, 47 mol.% KNO_3 and 410 K, 54 mol.% KNO_3.

Zhang X. et al. [24]The binary phase diagram of NaNO3-KNO3 was studied by differential scanning calorimetry (DSC) and high-temperature x-ray diffractometry. The solid solutions in the intermediate concentration phase appeared to be a mixture of the $NaNO_3$-based solid solutions and KNO_3-based solid solutions. This behaviour below the solidus suggests that

$NaNO_3$-KNO_3 might well be regarded as a system with limited solid solubility's instead of a continuous series of solid solutions. The temperatures for the solidus and liquidus have been determined by the author with consideration of limited terminal solid solutions. Two models, the Henrian solution and regular solution theory for $NaNO_3$-based phase and the KNO_3-based phase, respectively, were used by the author to reproduce the solidus and liquidus of the phase diagram. From the reported data by author the results are in good agreement with the DSC data. The thermodynamic properties for the $NaNO_3$-based and KNO_3-based solid solutions have been derived by the author from an optimization procedure using the experimental data. The calculated phase diagram and optimized thermodynamic parameters obtained by the author are thermodynamically self-consistent. Thus, the limited solid solution model seems to be more consistent with the phase diagram obtained by DSC than the continuous solid solution model.

Vallet C. [25] The liquidus curves of $LiNO_3$ + $AgNO_3$, $LiNO_3$ + $NaNO_3$, and $LiNO_3$- KNO_3 have been determined by the author in this paper. The excess Gibbs energies were computed by the author from the phase diagram has been compared with the excess enthalpies measured by Kleppa. The results reported by the author for $LiNO_3$-$AgNO_3$ system was found to be regular at all compositions. The interaction parameters are reported by author interpreted in terms of the Forland model with the assumption of three kinds of interaction between ions: Colombia, polarization, and London dispersion.

Yu-Ting W. et al. [26] In this work an experimental system of parabolic trough solar collector and heat transfer was set up by the author with a new molten salt employed as the heat transfer medium (with a melting point of 86 °C and a working temperature upper limit of 550 °C). The circulation of molten salts in the designed system by author took place over 1000 h. Experiments were conducted by author to obtain the heat loss of the Heat Collector Element (HCE), the total heat transfer coefficient of the water-to-salt heat exchanger, and the convective heat transfer coefficients for the low melting point molten salt in a circular tube. The results reported by author that the thermal loss of the tested HCE is higher than that of the PTR70, and the thermal loss at the joints of the collector tube represents about 5% of the total loss in the entire tube. The total heat transfer coefficient of the water-to-salt heat exchanger was reported by author in between 600 and 1200 W/(m^2.k) in the ranges of 10,000 < Re < 21,000 and 9.5 < Pr < 12.2. The experimental data reported by author show good

agreement with existing well-known correlations presented by the Sieder-Tate equation and the Gnielinski equation.

Christopher W.B. et al. [27] In this paper author proposed modifications to the standard interaction parameter formalism. The modified formalism, known as the "Unified Interaction Parameter Formalism," is discussed by the author in the present article with respect to thermodynamic consistency at finite concentrations in binary, ternary, and multicomponent systems. A new method was introduced by the author who is independent of integration paths, is proposed to derive the equations of the formalism by differentiation of the integral Gibbs energy expression. From the reported data by author, it is shown that the formalism is thermodynamically exact in both dilute and nondilute composition regions. It is also shown by author that the formalism reduces to Wagner's formalism at infinite dilution and to Darken's quadratic formalism in dilute solutions. Examples are presented by the author and methods are discussed for determining the parameters of the formalism from thermodynamic data.

Chapter 3

Mathematical Modeling

The determination of phase diagram, eutectic concentration and eutectic temperature can be determined by mathematical model or experimentation procedure. The determination of phase diagram with the help of experimentation is costly and time consuming. Therefore, in this study regular solution theory was used to determine the phase diagram, eutectic concentration and eutectic temperature of binary and ternary salt mixture.

3.1 Various Theories of Solutions Used to Determine Thermodynamic Properties of Salts.

According to Zumdahl [9], a solution is a homogeneous mixture of two or more components. Such a mixture constitutes of a solute which is dissolved in a solvent. The formation of a mixture introduces a Gibbs potential of mixing, expressed as

$$\Delta G = \Delta H - T\Delta S \tag{3.1}$$

Where ΔG signifies the difference in Gibbs potential when particles are in the solution and when in their reference state. The treatment of "mixture potentials" is what differences the various models presented in the following.

Solutions come in various forms, ranging from dilute solutions to molten salts and alloys. Dilute solutions have been studied extensively, both because of practical importance and the somewhat simple formalism arising from the idea that interactions between solute components can be disregarded. This approximation is however not valid in the opposite extreme, as inter ionic forces could contribute significantly. This is for instance the case for molten salts.

The term "Molten salt" is rather self-descriptive; it is a salt which is melted. For the Hall-Héroult cell, the main salt of interest is cryolite. The melting point of pure cryolite is 1284K, above which it becomes liquid and thus a molten salt. The molten salt thus behaves like a fluid, but has a significant microstructure due to the disassociated ions constituting the melt. The thermodynamic properties of molten salts

are somewhat more complicated than other solutions, due to the fact that there is no solvent.

The molten salt can be visualized as an array of positively and negatively charged cations and anions, similar to that found in solid crystals, though the structure can be significantly different. Due to the strong Coulomb repulsion between charges of same sign (and attractive if opposite) a cation will preferably have an anion as its nearest neighbour. As discussed in Grjotheim and Kvande [10], for a compound like NaCl, the energy required to transfer an anion from its preferred site to a site where it is surrounded by only anions requires energy of about 800kJ, approximately 30 times larger than the heat of melting of the compound. It is thus reasonable to assume that there are only two kinds of positions in a molten salt, one kind for cations and one kind for anions. This tendency towards ordering differs from ideal solutions, treated in the following.

3.1.1 Raoultian ideal solution theory

Ideal solutions are characterized by negligible interactions between particles. As shown in chapter 9 in Gaskell [11], a consequence of non-interacting particles is Raoult's law

$$a_i = X_i \tag{3.2}$$

stating that the activity [1] of the i-th component is equal to its mole fraction. The partial mixing Gibbs potential (of the i-th component) is thus given by

$$\Delta G_i = RTlna_i = RTlnX_i \tag{3.3}$$

Hence, for an ideal binary A-B solution, the Gibbs energy of mixing can be expressed as

$$\Delta G^{id} = RT(X_A lnX_A + X_B lnX_B) \tag{3.4}$$

The assumption of non-interacting particles implies that they should be distributed randomly in the solution. Hence, the entropy of mixing for a binary A-B solution can be expressed as

$$\Delta S' = k\frac{(N_A+N_B)!}{N_A!N_B!} \tag{3.5}$$

Using Stirling's approximation and division with the total mole number, the following expression is obtained

$$\Delta S = -R(X_A lnX_A + X_B lnX_B) \tag{3.6}$$

Comparison with equation 3.1 shows that the enthalpy of mixing, ΔH, is zero for ideal solutions.

Due to the simple mathematical relations for ideal solutions, models based on this assumption are widely used and constitute the basics for the so called Temkin activity model [13]. According to Grjotheim and Kvande [10], this formalism has proved to be very useful in approximate calculations of thermodynamic properties of molten salts.

3.1.2 Deviation from Ideality

Following Gaskell [11], a non-ideal solution is one in which the activities of the components are not equal to their mole fractions. However, as substantial work has been done on ideal models, it is useful to model non-ideality as a modification of ideality. This is done by introducing the activity coefficient, defined by

$$\Upsilon_i = \frac{a_i}{X_i} \tag{3.7}$$

For ideal solutions, γ_i is unity yielding Raoult's law. Solutions with $\gamma_i > 1$ are said to have a positive deviation from Raoult's law, while $\gamma_i < 1$ signifies a negative deviation. The Gibbs energy of mixing for a non-ideal binary solution can thus be expressed as

$$\Delta G = RT(X_A lna_A + X_B lna_B) = RT(X_A ln\Upsilon_A + X_B ln\Upsilon_B + X_A lnX_A + X_B lnX_B) \tag{3.8}$$

$$= \Delta G^{id} + \Delta G^{xs} \tag{3.9}$$

where ΔG^{XS} is the excess Gibbs potential, incorporating the entire nonideal behaviour. If the activity coefficient is allowed to be temperature dependent, it is readily observed from the Gibbs-Helmholtz equation that nonzero enthalpies of mixing are possible, as

$$\frac{\partial \Delta G_i/T}{\partial T} = \frac{\partial R ln\Upsilon_i}{\partial T} = -\frac{\Delta H_i}{T^2} \tag{3.10}$$

3.1.3 Regular Solution Theory

Hildebrand [12] defines a regular solution as one where

$$\Delta H_i \neq 0 \tag{3.11}$$

and

$$\Delta S_i = \Delta S_i^{id} = -RlnX_i \tag{3.12}$$

The excess Gibbs potential is thus related to the enthalpy of mixing in a straightforward manner

$$\Delta G^{xs} = \Delta H \tag{3.13}$$

Expanding the activity coefficient up to second order in mole fractions, Hildebrand [12] found the following relation for activity coefficients in binary systems

$$RTln\gamma_B = \alpha X_A^2 \tag{3.14}$$

$$RTln\gamma_A = \alpha X_B^2 \tag{3.15}$$

where α is a constant. Using the regular expansion model, the excess Gibbs potential (and thus the enthalpy of mixing) reduces to

$$\Delta G^{xs} = \Delta H = \alpha X_A X_B \tag{3.16}$$

where the mass balance $X_A + X_B = 1$ has been used. Equation 3.13 shows that the excess Gibbs potential and enthalpy of mixing is temperature independent for the regular model.

Regular solution models assume a random distribution of atoms even though the enthalpy of mixing is nonzero. In reality, a random solution is expected only if interactions between particles is negligible or at so high temperatures that the entropy term overwhelms any tendency for ordering of atoms.

3.1.4 Subregular Solution Theory

The subregular model is a further extension of the regular model, allowing α to be composition dependent and ΔG^{XS} to depend on temperature. Following Gaskell [11].

$$\alpha = \alpha_0 + \alpha_1 X_B \tag{3.17}$$

and

$$\Delta G^{xs} = (\alpha_0 + \alpha_1 X_B)\, X_A X_B \left(1 - \frac{T}{\zeta}\right) \tag{3.18}$$

yielding

$$\Delta S^{xs} = \frac{(\alpha_0 + \alpha_1 X_B)\, X_A X_B}{\zeta} \equiv = (s_0 + s_1 X_B)\, X_A X_B \tag{3.19}$$

and

$$\Delta H = \Delta G^{xs} + \Delta S^{xs} = (\alpha_0 + \alpha_1 X_B)\, X_A X_B \equiv (h_0 + h_1 X_B)\, X_A X_B \tag{3.20}$$

From the above explained theory, the regular solution theory was used to determine the phase diagram, eutectic concentration and eutectic temperature of binary and ternary salt mixture. The procedure and resultant equations obtained after deriving basic equations of regular solution theory is explained as follows.

3.2 Mathematical Formulation of Binary System

The liquidus temperature of binary system is calculated using the equations derived on the basis of Regular solution theory [22]. Let us consider a binary system consisting of components A and B. The Gibbs free energy of component A can be expressed as

$$\Delta G^{A} = (\Delta H_A - T\Delta S_A) + (\Delta H_m^{Al} - T\Delta S_m^{Al}) - (\Delta H_m^{As} - T\Delta S_m^{As}) \tag{3.21}$$

The Gibbs free energy of component A will be zero when the liquid and solid solution of component A are in thermodynamic equilibrium. Therefore, under thermodynamic equilibrium condition, Eq. (3.21) is reduced to

$$(\Delta H_A - T\Delta S_A) + (\Delta H_m^{Al} - T\Delta S_m^{Al}) - (\Delta H_m^{As} - T\Delta S_m^{As}) = 0 \tag{3.22}$$

In Eq. (3.22), the first term denotes the free energy of fusion, the second term denotes the partial molar energy of mixing of liquid solution and third term represents the partial molar energy of mixing of solid solution.

The ΔH_A and ΔS_A in first term of Eq.(3.22) is estimated using the expressions as given below

$$\Delta H_A = \Delta H_f - \int_T^{T_M} (C_{Pl}^A - C_{Ps}^A) dT \tag{3.23}$$

and

$$\Delta S_A = \Delta S_f - \int_T^{T_M} \frac{(C_{Pl}^A - C_{Ps}^A) dT}{T} \tag{3.24}$$

Where ΔH_f^A and ΔS_f^A represent enthalpy and entropy of fusion of component A at its melting point. The C_{Ps}^A and C_{Pl}^A represent specific heat of component A in solid and liquid phase respectively. The above physical parameters are given in Table 3.1.

In Eq. (3.22), the partial entropy of mixing, ΔS_m^A , for liquid and solid phase are estimated using the expressions as given below

$$\Delta S_m^A = -Rlnx_A \tag{3.25}$$

where x_A represent mole fraction of component A in either liquid part or solid part of liquid-solid mixture.

Table 3.1: Physical parameters for the single salts

Salt	Molar Mass (g mol^{-1})	Melting Temperature (Kelvin)	Latent Heat (J g^{-1})	Cp(l) - Cp(s) (J g^{-1} K^{-1})
$NaNO_3$	84.9947	577.5	173	-0.11
KNO_3	101.103	607.4	96.6	-0.03
$LiNO_3$	68.946	525.9	363	0.25

In Eq. (3.22), the partial enthalpy of mixing, ΔH_m^A , for liquid and solid phase are estimated using the Gibbs- Duhem equation as given below

$$\Delta H_m^A = \Delta H_m + (1 - x_A)\frac{d\Delta H_m}{dx_A} \tag{3.26}$$

where ΔH_m is enthalpy of mixing which is estimated using the following expression

$$\Delta H_m = x_A x_B(a + bx_A + cx_A x_B) \tag{3.27}$$

where a, b, and c are the empirical coefficients. The empirical coefficients for liquid phase and solid phase were experimentally derived by Kleppa[28] and Kramer[22] respectively. These coefficients are given in Table 3.2.

Table 3.2: Empirical coefficients of liquid and solid phase for each of the binary systems

	ΔH_m, liquid			ΔH_m, solid		
	a	B	C	a	B	C
$NaNO_3$:KNO_3	-1707	-284	0	6276	0	0
$LiNO_3$:$NaNO_3$	-1941	-2928	0	9204	3347	0
$LiNO_3$:KNO_3	-9183	-364	-1937	10,460	4184	0

Using Eqs. (3.22) to (3.27), the Gibbs free energy equation for component A can be finally expressed as

$$\left(1 - \frac{T}{T_M^A}\right)\Delta H_f^A + \Delta C_{PA}\left[T - T_M^A - Tln\frac{T}{T_M^A}\right] + RT\left(lnx_A^l - lnx_A^s\right)$$
$$+ \left(a_l\left(x_B^l\right)^2 + 2b_l x_A^l\left(x_B^l\right)^2 + 2c_l x_A^l\left(x_B^l\right)^3 - c_l\left(x_A^l\right)^2\left(x_B^l\right)^2\right) - (a_s(x_B^s)^2 + 2b_s x_A^s(x_B^s)^2 +$$
$$2c_s x_A^s(x_B^s)^3 - c_s(x_A^s)^2(x_B^s)^2) = 0 \tag{3.28}$$

Similarly, the Gibbs free energy equation for component B can be written as

$$\left(1-\frac{T}{T_M^B}\right)\Delta H_f^B+\Delta C_{PB}\left[T-T_M^B-Tln\frac{T}{T_M^B}\right]+RT\left(lnx_B^l-lnx_B^s\right)$$
$$+\left(a_l\left(x_A^l\right)^2+b_l\left(x_A^l\right)^3-b_l\left(x_A^l\right)^2x_B^l-2c_l\left(x_A^l\right)^3x_B^l-c_l\left(x_A^l\right)^2\left(x_B^l\right)^2\right)-(a_s(x_A^s)^2+$$
$$b_s(x_A^s)^3-b_s(x_A^s)^2x_B^s-2c_s(x_A^s)^3x_B^s-c_s(x_A^s)^2(x_B^s)^2)=0 \quad (3.29)$$

The two more equations for mole fraction of components A and B in liquid and solid phase can be written as

$$x_A^l+x_B^l=1 \quad (3.30)$$

and

$$x_A^s+x_B^s=1 \quad (3.31)$$

The Eqs. (3.28) - (3.31) must be satisfied simultaneously at a given composition of binary mixture. There are five unknowns and only four equations. Therefore, the composition of one of the salt must be known in advance and rest of the four unknowns are obtained by solving Eqs. (3.28) - (3.31). Finally, simultaneous solution of these equations provide values of liquid and solid compositions for both of the components and the temperature at that composition.

3.3 Mathematical Modeling of Ternary System

Let us consider a ternary system consisting of components A, B and C. Again, as in case of binary system, the Gibbs free energy of each of the components in a ternary system will be zero when the liquid and solid solution of these components are in thermodynamic equilibrium. The free energy of fusion, as represented by first term in Eq. (3.32), for ternary system is estimated in the similar fashion as in case of binary system. However, determination of partial enthalpy of mixing for each component in case of ternary system is a bit complicated due to the interaction between all the three salt components. The enthalpy of mixing can be expressed as the summation of three binary mixing interactions and one ternary interaction. In this model the ternary interaction is assumed negligible as compared to the binary interactions. Thus the enthalpy of mixing in liquid and solid phase for ternary system is estimated using the following expression.

$$\Delta H_m=\Delta H_m^{A-B}+\Delta H_m^{B-C}+\Delta H_m^{C-A} \quad (3.32)$$

Using Eq. (7) the above expression leads to,

$$\Delta H_m=(a_1x_Ax_B+b_1x_A^2x_B+c_1x_A^2x_B^2)+(a_2x_Bx_C+b_2x_C^2x_B+c_2x_C^2x_B^2)+$$
$$(a_3x_Ax_C+b_3x_C^2x_A+c_3x_C^2x_A^2) \quad (3.33)$$

The empirical coefficients in above Eq. (3.28) are similar to those used in binary system. Again, the Gibbs-Duhem equation, as given by Eq. (3.26), is utilized to estimate the partial enthalpy of each of the components in both liquid and solid phase.

Finally, the Gibbs free energy for each of the components can be expressed as given below

For component A

$$\left(1-\frac{T}{T_M^A}\right)\Delta H_f^A+\Delta C_{PA}\left[T-T_M^A-Tln\frac{T}{T_M^A}\right]+RT\left(lnx_A^l-lnx_A^s\right)+\Big(\left(1-x_A^l\right)\Big[a_{1l}x_B^l+2b_{1l}x_A^lx_B^l+2c_{1l}x_A^l\left(x_B^l\right)^2+a_{3l}x_C^l+b_{3l}\left(x_C^l\right)^2+2C_{3l}x_A^l\left(x_C^l\right)^2\Big]-c_{1l}\left(x_A^l\right)^2\left(x_B^l\right)^2-3c_{2l}\left(x_C^l\right)^2\left(x_B^l\right)^2-a_{2l}x_B^lx_C^l-2b_{2l}x_B^l\left(x_C^l\right)^2-b_{3l}x_A^l\left(x_C^l\right)^2-c_{3l}\left(x_A^l\right)^2\left(x_C^l\right)^2\Big)-\big((1-x_A^s)[a_{1s}x_B^s+2b_{1s}x_A^sx_B^s+2c_{1s}x_A^s(x_B^s)^2+a_{3s}x_C^s+b_{3s}(x_C^s)^2+2c_{3s}x_A^s(x_C^s)^2]-c_{1s}(x_A^s)^2(x_B^s)^2-3c_{2s}(x_C^s)^2(x_B^s)^2-a_{2s}x_B^sx_C^s-2b_{2s}x_B^s(x_C^s)^2-b_{3s}x_A^s(x_C^s)^2-c_{3s}(x_A^s)^2(x_C^s)^2\big)=0 \tag{3.34}$$

For component B

$$\left(1-\frac{T}{T_M^B}\right)\Delta H_f^B+\Delta C_{PB}\left[T-T_M^B-Tln\frac{T}{T_M^B}\right]+RT\left(lnx_B^l-lnx_B^s\right)+\Big(\left(1-x_B^l\right)\Big[a_{1l}x_A^l+b_{1l}\left(x_A^l\right)^2+a_{2l}x_C^l+b_{2l}\left(x_C^l\right)^2+2c_{2l}x_B^l\left(x_C^l\right)^2+2c_{1l}x_B^l\left(x_A^l\right)^2\Big]-b_{1l}\left(x_A^l\right)^2x_B^l-c_{1l}\left(x_A^l\right)^2\left(x_B^l\right)^2-3c_{3l}\left(x_A^l\right)^2\left(x_C^l\right)^2-b_{2l}x_B^l\left(x_C^l\right)^2-c_{2l}\left(x_B^l\right)^2\left(x_C^l\right)^2-a_{3l}x_A^l\left(x_C^l\right)^2+2b_{3l}\left(x_C^l\right)^2x_C^l\Big)-\big((1-x_B^s)[a_{1s}x_A^s+b_{1s}(x_A^s)^2+a_{2s}x_C^s+b_{2s}(x_C^s)^2+2c_{2s}x_B^s(x_C^s)^2+2c_{1s}x_B^s(x_A^s)^2]-b_{1s}(x_A^s)^2x_B^s-c_{1s}(x_A^s)^2(x_B^s)^2-3c_{3s}(x_A^s)^2(x_C^s)^2-b_{2s}x_B^s(x_C^s)^2-c_{2s}(x_B^s)^2(x_C^s)^2-a_{3s}x_A^s(x_C^s)^2+2b_{3s}(x_C^s)^2x_C^s\big)=0 \tag{3.35}$$

For component C

$$\left(1-\frac{T}{T_M^C}\right)\Delta H_f^C+\Delta C_{PC}\left[T-T_M^C-Tln\frac{T}{T_M^C}\right]+RT\left(lnx_C^l-lnx_C^s\right)+\Big(\left(1-x_C^l\right)\Big[a_{2l}x_C^l+2b_{2l}x_B^lx_C^l+2c_{2l}x_C^l\left(x_B^l\right)^2+a_{3l}x_A^l+2b_{3l}x_A^lx_C^l+2c_{3l}x_c^l\left(x_A^l\right)^2\Big]-3c_{1l}\left(x_A^l\right)^2\left(x_B^l\right)^2-c_{3l}\left(x_A^l\right)^2\left(x_C^l\right)^2-a_{1l}x_A^lx_B^l-2b_{1l}x_B^l\left(x_A^l\right)^2-c_{2l}\left(x_B^l\right)^2\left(x_C^l\right)^2\Big)-\big((1-x_C^s)[a_{2s}x_C^s+2b_{2s}x_B^sx_C^s+2c_{2s}x_C^s(x_B^s)^2+a_{3s}x_A^s+2b_{3s}x_A^sx_C^s+2c_{3s}x_c^s(x_A^s)^2]-3c_{1s}(x_A^s)^2(x_B^s)^2-c_{3s}(x_A^s)^2(x_C^s)^2-a_{1s}x_A^sx_B^s-2b_{1s}x_B^s(x_A^s)^2-c_{2s}(x_B^s)^2(x_C^s)^2\big)=0 \tag{3.36}$$

The two more equations based on relation among composition of components in both liquid and solid phase can be written as

$$x_A^l+x_B^l+x_C^l=1 \tag{3.37}$$

and

$$x_A^S + x_B^S + x_C^S = 1 \tag{3.38}$$

At any given composition of ternary system, the five equations represented by Eqs. (3.34) - (3.38) must be satisfied simultaneously. These five equations have seven unknowns. Therefore, the composition of two of the components of ternary is assumed to find rest of the five unknowns by solving Eqs. (3.34) - (3.38). Finally, simultaneous solution of these equations provides values of liquid and solid compositions of each of the components and the temperature at that composition.

Chapter 4

Sample Preparation and Experimental Work

4.1 Sample Preparation

4.1.1 Preparation of $NaNO_3$- KNO_3 Salt Mixture

In this work $NaNO_3$ (Purity higher than 99 wt. %), KNO_3 (Purity higher than 99 wt. %) from chemical company named "Loba-Chemie" were used to prepare binary salt mixture without further purification. The equipment, "CAS CAUW 2200" shown in figure 4.1 was used to measure the weight of salts. This analytical balance has an accuracy of 0.01 mg.

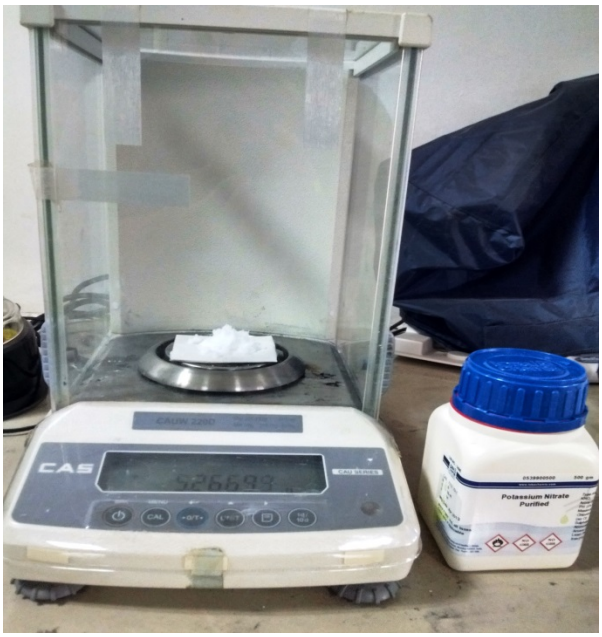

Figure 4.1: Measuring weight of KNO_3

An amount of 50 g of salt was taken and heated at a temperature of 120°C in an electric oven for 24 hour to remove every trace of moisture which could be previously present in salt packaging. These completely anhydrous salts were measured and mixed together to form binary mixture having eutectic composition. The salt mixtures were then taken, thoroughly grinded and mixed together with the help of mechanical grinder shown in figure 4.2 to form homogeneous mixture. Since, nitrate salts are hygroscopic in nature, so they have a tendency to gain moisture from environment during grinding and mixing process. Therefore the mixture of

Figure 4.2: Mixing of salts at eutectic mixture

binary nitrate was again heated to 120°C for 24 hour shown in figure 4.3. Finally the prepared mixture was kept in the sealed containers and then the sealed container was kept in air tight box filled with silica gel desiccant.

Figure 4.3: Heating of salt to evaporate moisture

4.1.2 Preparation of $LiNO_3$- KNO_3 Salt Mixture

In this work $LiNO_3$ (Purity higher than 98 wt % figure 4.4), KNO_3 (Purity higher than 99 wt % figure 4.5) from chemical company named “Loba-Chemie” were used to prepare binary salt mixture without further purification. The equipment, “CAS CAUW 2200” shown in figure 4.6 was used to measure the weight of salts. This analytical balance has an accuracy of 0.01 mg.

Figure 4.4: 500g packaging of $LiNO_3$ salt

An amount of 50 g of salt was taken and heated at a temperature of 120°C in an electric oven for 24 hour to remove every trace of moisture which could be previously present in salt packaging. These completely anhydrous salts were measured and mixed together to form binary mixture having eutectic composition. The salt mixtures were then taken, thoroughly grinded and mixed together with the help of mechanical grinder to form homogeneous mixture. Since, nitrate salts are hygroscopic in nature, so they have a tendency to gain moisture from environment during grinding and mixing process.

Figure 4.5: 500g packaging of KNO_3 salt

Therefore the mixture of binary nitrate was again heated to 120°C for 24 hour. Finally the prepared mixture was kept in the sealed containers and then the sealed container was kept in air tight box filled with silica gel desiccant.

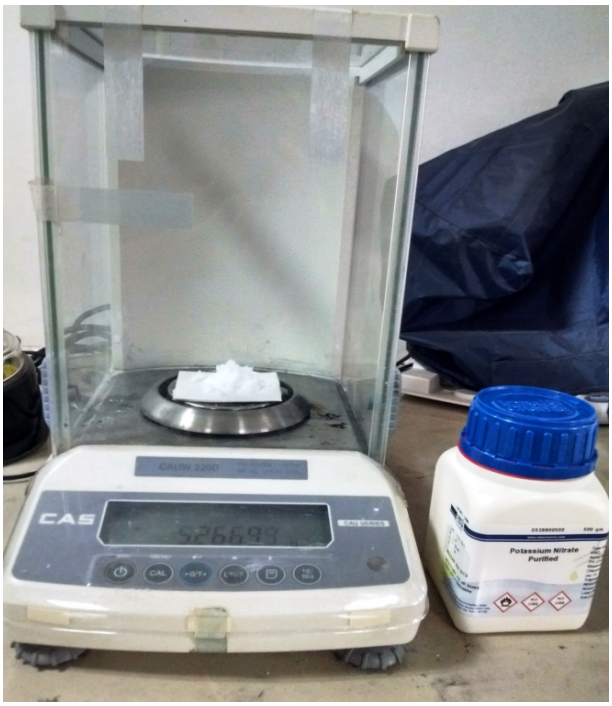

Figure 4.6: Measuring weight of $NaNO_3$

4.1.3 Preparation of $LiNO_3$ - $NaNO_3$ Salt Mixture

In this work $LiNO_3$ (Purity higher than 98 wt. %), $NaNO_3$ (Purity higher than 99 wt. %) from chemical company named "Loba- Chemie" were used to prepare binary salt mixture without further purification. The equipment, "CAS CAUW 2200" shown in figure 4.9 was used to measure the weight of salts. This analytical balance has an accuracy of 0.01 mg. An amount of 50 g of salt was taken and heated at a temperature of 120°C in an electric oven for 24 hour to remove every trace of moisture which could be previously present in salt packaging. These completely anhydrous salts were measured and mixed together to form binary mixture having eutectic composition. The salt mixtures were then taken, thoroughly grinded and mixed together with the help of mechanical grinder shown in figure 4.7 to form homogeneous mixture. Since, nitrate salts are hygroscopic in nature, so they have a tendency to gain moisture from environment during grinding and mixing process. Therefore the mixture of binary nitrate was again heated to 120°C for 24 hour. Finally the prepared mixture was kept in the sealed.

Figure 4.7: Mixing of salts at eutectic mixture

containers and then the sealed container was kept in air tight box filled with silica gel desiccant.

Figure 4.8: 500g packaging of $NaNO_3$ salt

4.1.4 Preparation of $LiNO_3$-$NaNO_3$-KNO_3 Salt Mixture

In this work $NaNO_3$ (Purity higher than 99 wt %), KNO_3 (Purity higher than 99 wt %) and $LiNO_3$ (Purity higher than 98 wt %) from chemical company named "Loba-Chemie" were used to prepare ternary salt mixture without further purification. The equipment, "CAS CAUW 2200" was used to measure the weight of salts. This analytical balance has an accuracy of 0.01 mg.

Figure 4.9: Measuring weight of $NaNO_3$

An amount of 50 g of each salt was taken and heated at a temperature of 120^0C in an electric oven for 24 hour to remove every trace of moisture which could be previously present in salt packaging. These completely anhydrous salts were measured and mixed together to form a ternary mixture having eutectic composition. The salt mixture was then taken, thoroughly grinded and mixed together with the help of mechanical grinder to form homogeneous mixture. Since, nitrate salts are hygroscopic in nature, so they have a tendency to gain moisture from environment during grinding and mixing process. Therefore the mixture of nitrates was again heated to 120°C for 24 hour shown in figure in 4.10. Finally the prepared mixture was kept in the sealed containers depicted in figure 4.11 and then the sealed containers were kept in air tight box filled with silica gel desiccant.

4.2 Experimentation

The phase transition temperature at eutectic concentration of binary and ternary salt systems was experimentally determined by using TG/DTA (EXSTAR SII 6300) facility. The TG/DTA facility was used to obtain thermal gravimetric signal (TG) and differential scanning calorimetric signal (DSC) for binary and ternary salt systems. The instrument has horizontal differential type weight balance that uses alumina powder (5.5 mg) as reference weight during thermal analysis. The crucible of the instrument was made of alumina and has a pan volume of 45µL. The experiments were conducted by taking a sample of 5.4 -5.6 mg of the salt mixture in the crucible, then the sample was heated from ambient temperature to 615°C with heating rate of 10°C /min. Each of the experiments was conducted in an inert atmosphere of nitrogen, which was supplied to the instrument at rate of 200ml/min. The setup was displayed in figure 4.12.

Figure 4.10: Heating of salt to evaporate moisture

Figure 4.11: Sealed containers filled with sample of salt mixture

Thermogravimetric Analysis (TGA) instrument is used to measures the amount and rate of change in the weight of a material as a function of temperature or time in a controlled atmosphere. Measurements are used primarily to determine the composition of materials and to predict their thermal stability at temperatures up to 1200°C. The technique can characterize materials that exhibit weight loss or gain due to decomposition, oxidation, or dehydration. TGA can utilized to find out the following objectives

1. Estimated Lifetime of a Product
2. Moisture and Volatiles Content of Materials

3. Thermal Stability of Materials
4. Decomposition Kinetics of Materials
5. Oxidative Stability of Materials
6. The Effect of Reactive or Corrosive Atmospheres on Materials
7. Composition of Multi-component Systems

The thermal stability of the salts under investigation was determined by carrying out thermal gravimetric analysis using TG/DTA (EXSTAR SII 6300) instrument. The process of thermal gravimetric analysis was carried out simultaneously during the process of determining the phase transition temperature of binary and ternary mixtures of salt.

Figure 4.12**:** TG/DTA (EXSTAR SII 6300) facility at IIT Roorkee

Chapter 5

Result and Discussion

5.1 Binary System Results

A computer program was written in MATLAB to solve the equations of mathematical model in order to predict the eutectic concentration, phase transition temperature and phase diagram of binary and ternary salt mixtures. The results obtained from mathematical model and experimental work are presented in this section.

The results obtained from mathematical model were used to draw phase diagram of $NaNO_3$-KNO_3 binary system and it is displayed in Figure 5.1. The theoretical phase diagram, as shown in Figure 5.1, is also compared with the experimental work done by Zhang[24]. The figure shows that the mathematical model predicts the eutectic temperature of 220.34°C at a eutectic composition of 52 mol. % KNO_3 and 48 mol. % $NaNO_3$. It can also be seen that the predicted results obtained for liquidus curve are in good agreement with the experimental data of Zhang[24]. However, there is a little deviation in the predicted data obtained for solidus curve with the experimental data reported by Zhang[24].

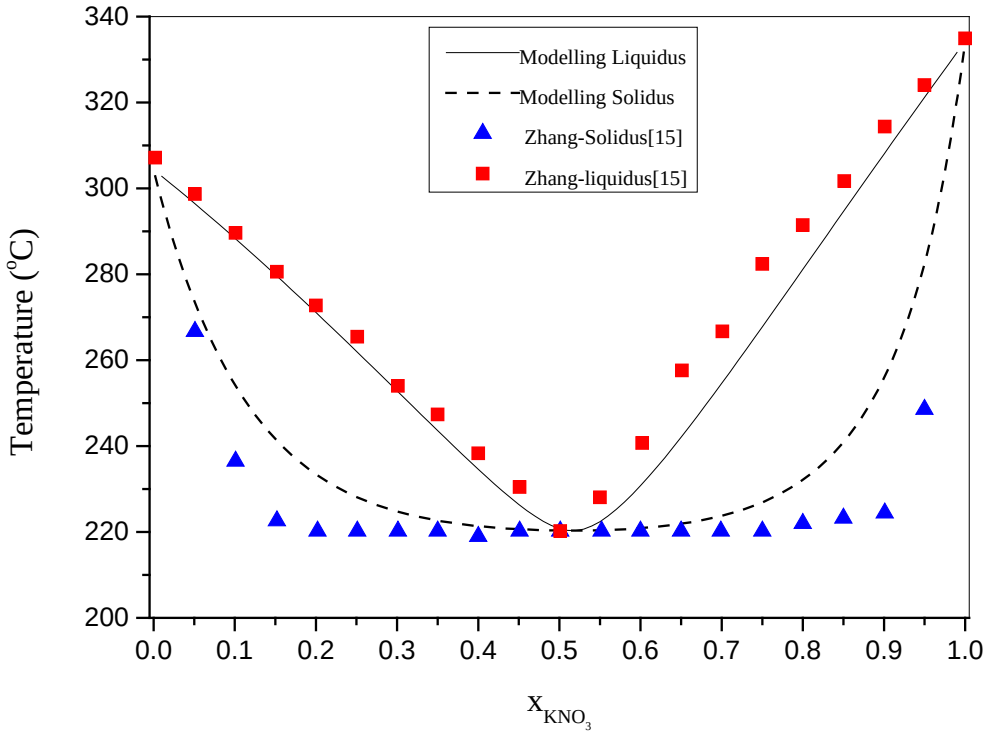

Figure 5.1**:** Comparison of theoretical phase diagram of $NaNO_3$-KNO_3 binary system with the experimental data of Zhang[24].

The results obtained from deferential scanning calorimetry (DSC) and thermogravimetric analysis (TG) of $NaNO_3$-KNO_3 salt mixture are shown in Figure 5.2. It can be seen that the eutectic temperature of $NaNO_3$-KNO_3 salt mixture was found to be 221°C. The results obtained from TG shows that the weight percent of the eutectic mixture of $NaNO_3$-KNO_3 is found to be 98% at 570°C. Therefore, it can be said that eutectic mixture of $NaNO_3$-KNO_3 is thermally stable up to a temperature of a 570°C.

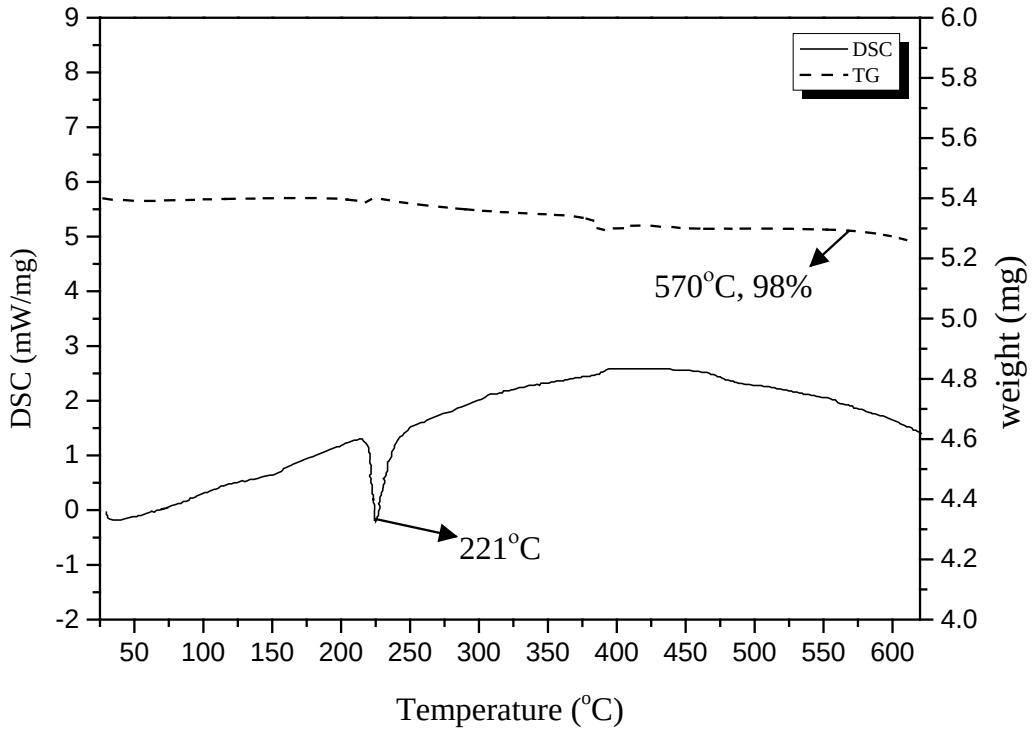

Figure 5.2: TG and DSC curves of eutectic mixture of $NaNO_3$-KNO_3 binary salt

The phase diagram obtained from thermodynamic model for $NaNO_3$-$LiNO_3$ binary salt system is shown in Figure 5.3. The eutectic phase transition temperature obtained from simulation is 184.14°C at a composition of 54 mol. % $LiNO_3$ and 46 mol. % $NaNO_3$. The figure also shows that the simulation results of $NaNO_3$-$LiNO_3$ binary salt system are in good agreement with the experimental data reported by Campbell et al. [29] and Vallet [25]. The predicted eutectic composition for $LiNO_3$-$NaNO_3$ binary system obtained from thermodynamic model is $x_{NaNO_3} = 0.46$ which exactly matches with the eutectic composition determined experimentally by Vallet [25]. However, at this eutectic composition, the eutectic phase transition temperature obtained from thermodynamic model and reported by Vallet [25] is 184.14°C and 193.8°C respectively.

Figure 5.4 shows the differential scanning calorimetry (DSC) and thermogravimetric (TG) analysis of $LiNO_3$-$NaNO_3$ salt mixture. Since $LiNO_3$ is highly hygroscopic in nature,

therefore it can be observed from Figure 5.4 that there is an initial weight loss (3% by wt.) which represents the water loss from the mixture. The results obtained from TG for $LiNO_3$-$NaNO_3$ binary salt system shows that the salt started dissociating at temperature of 510°C and can be used for short period up to a temperature of 554°C.

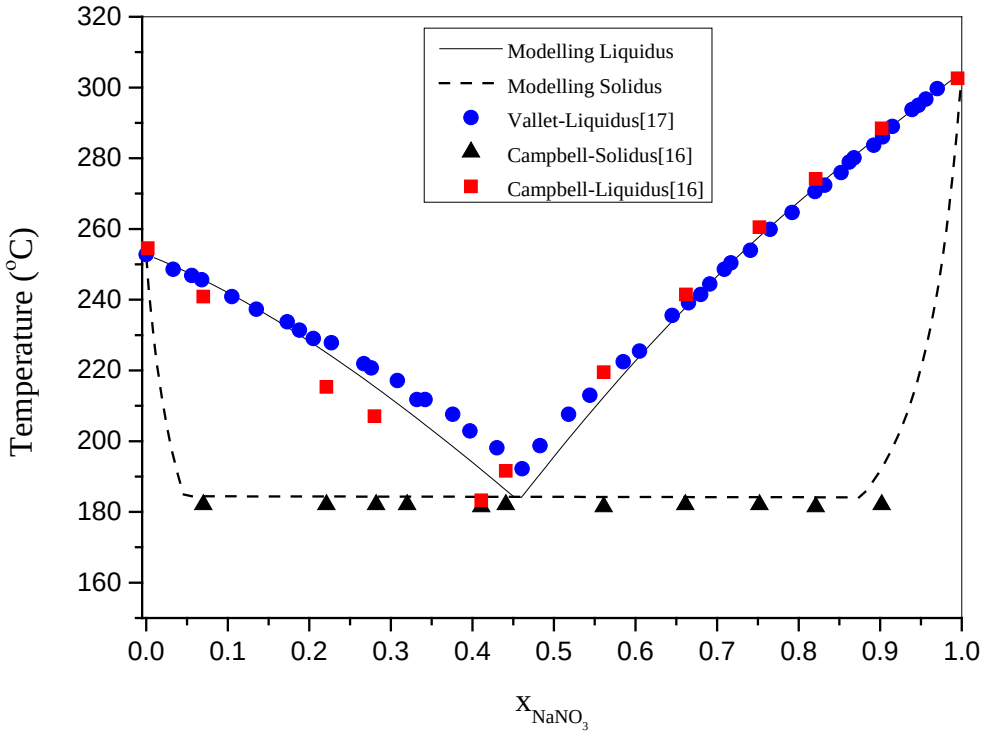

Figure 5.3: Comparison of theoretical phase diagram of $LiNO_3$-$NaNO_3$ binary system with the experimental data of Campbell et al [29] and Vallet [25].

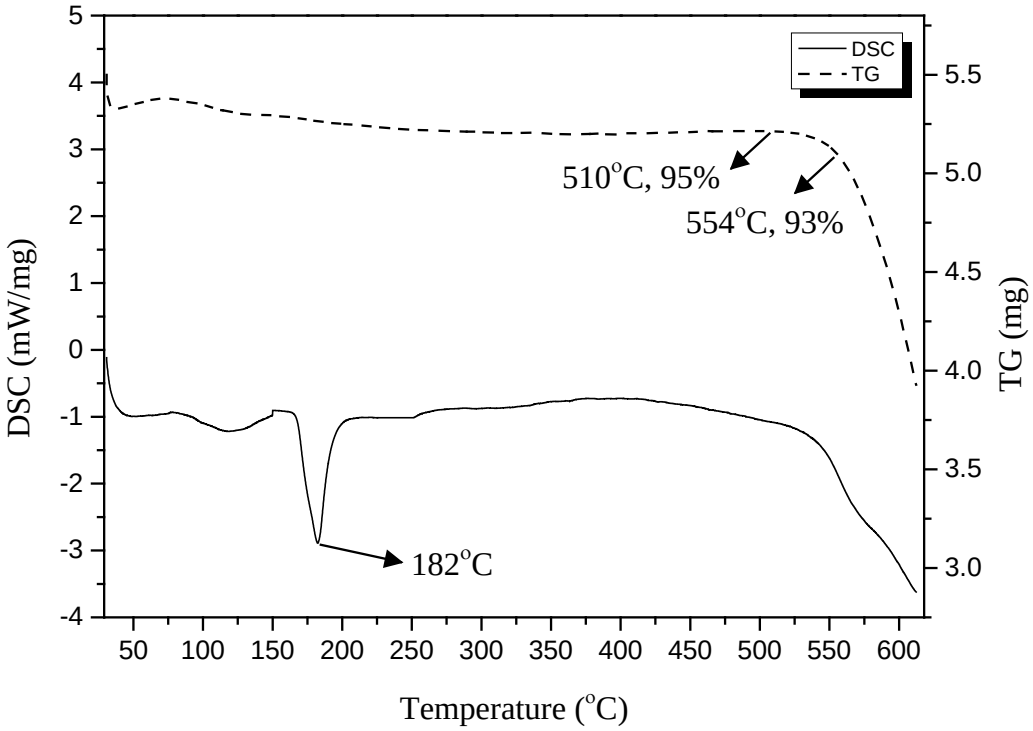

Figure 5.4: TG and DSC curves of eutectic mixture of $LiNO_3$-$NaNO_3$ binary salt

The DSC curve shows that the eutectic temperature of $LiNO_3$-$NaNO_3$ salt mixture is found to be 182°C. Whereas, the eutectic temperature of the same salt mixture as reported by Vallet [25] is 193.8°C. The reason for the difference between the present and previously reported values of eutectic temperature of $LiNO_3$-$NaNO_3$ binary system may be attributed to the fact of constantly mixed systems and observational technique was used by Vallet [25], whereas DSC is used in the present experimental work to determine the eutectic temperature.

The phase diagram for $LiNO_3$-KNO_3 binary salt system drawn from the results obtained from thermodynamic modeling is depicted in Figure 5.5. The eutectic phase transition temperature is calculated to be 123.92°C at a composition of 44 mol. % $LiNO_3$ and 56 mol. % KNO_3 respectively. The solidus line is seen to has a zero slope from 1 mol. % to 95 mol. % of KNO_3. It can be noticed that the predicted values for liquidus line of $LiNO_3$-KNO_3 binary system are in good agreement with the experimental data reported by Vallet[25] and Zhang et. al.[23]. However, there is deviation between the predicted values and experimental data reported by Zhang et al.[23] for solidus line of $LiNO_3$-KNO_3 binary system.

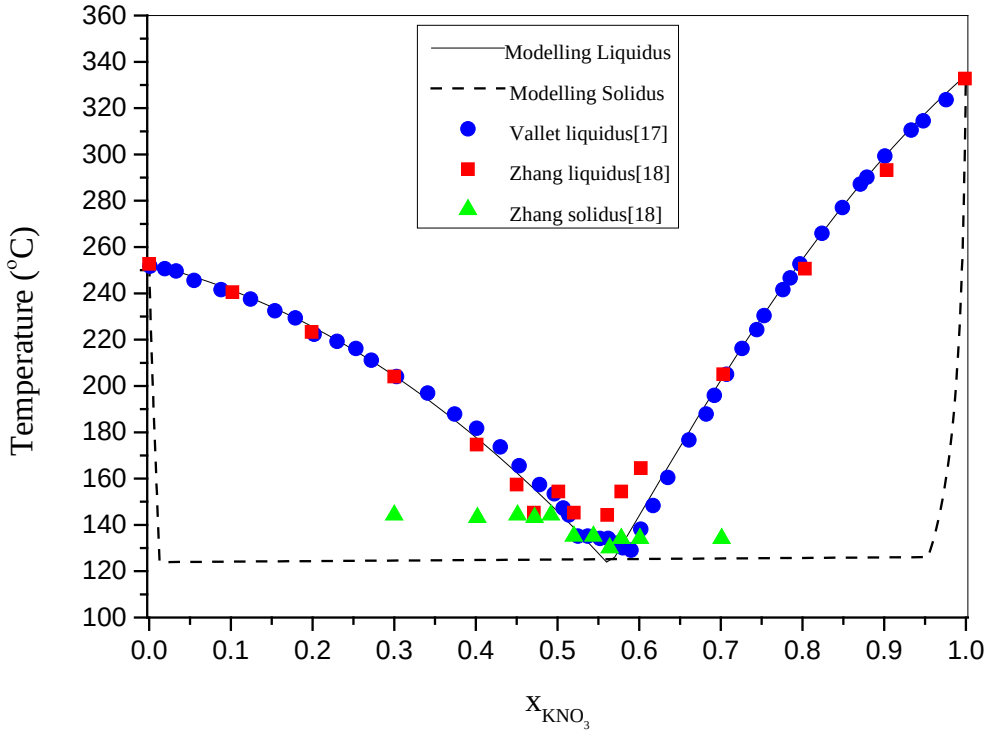

Figure 5.5: Comparison of theoretical phase diagram of $LiNO_3$-KNO_3 binary system with the experimental data of Vallet[25] and Zhang et. al.[23].

The results of TG and DSC curves for decomposition of eutectic mixture of $LiNO_3$-KNO_3 binary salt system is depicted in Figure 5.6. The melting point at eutectic composition

for $LiNO_3$-KNO_3 binary system is experimentally determined to be 126.5°C which is quite close to the value predicted by our thermodynamic model. The TG analysis of $LiNO_3$-KNO_3 salt mixture shows that the mixture starts dissociating at temperature of 514°C and can be used up to 564°C for short period of time.

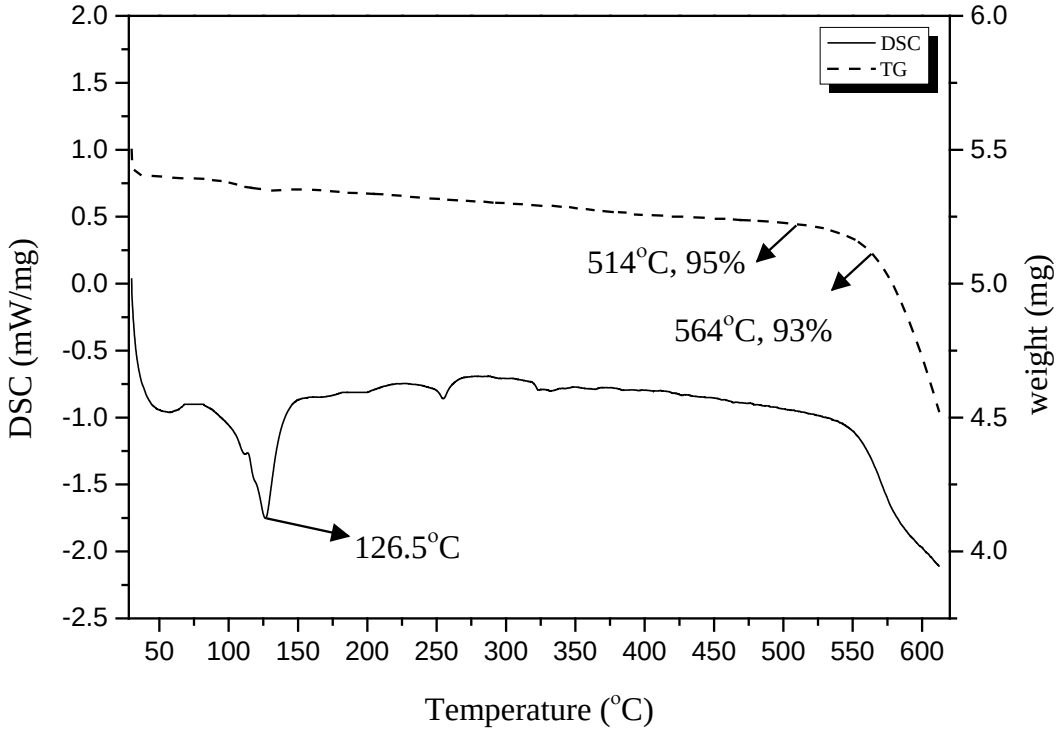

Figure 5.6: TG and DSC curves of eutectic mixture of $LiNO_3$-KNO_3 binary salt system.

5.2 Ternary System Results

The liquidus line of $LiNO_3$-$NaNO_3$-KNO_3 ternary system obtained from thermodynamic model at various concentration of $LiNO_3$ is depicted in Figure 5.7. The experimental results reported by Coscia [21] are compared with those predicted by the model. It can be noticed that the predicted results closely matches with the experimental data reported by Coscia [21]. The results obtained from mathematical model are in agreement with the previously reported fact that increasing the concentration of $LiNO_3$ decreases the melting temperature of the ternary mixture up until 38 mol. % $LiNO_3$ and further on increasing the concentration of $LiNO_3$ beyond 38 mol. % $LiNO_3$, the melting point of $LiNO_3$-$NaNO_3$-KNO_3 starts increasing.

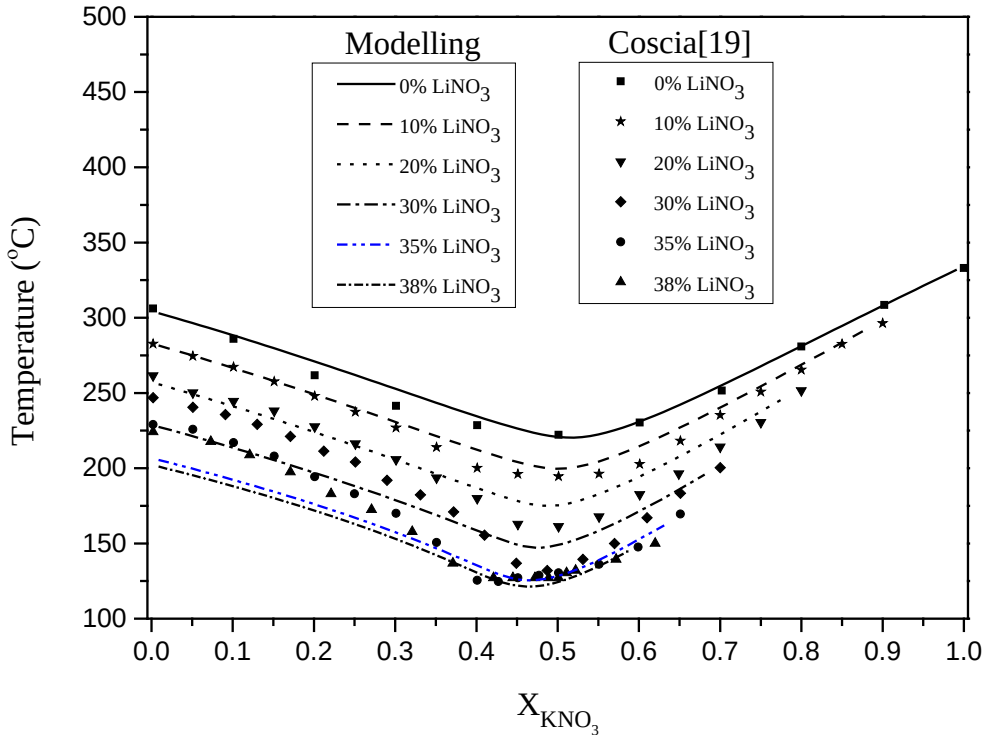

Figure 5.7: Comparison of liquidus line of $LiNO_3$-$NaNO_3$-KNO_3 system obtained from mathematical model with the experimental data of Coscia[21].

Coscia[21] reported that the $LiNO_3$-$NaNO_3$-KNO_3 ternary mixture with composition of KNO_3 between 40-50 mol. % and composition of $LiNO_3$ between 35-38 mol. % had a similar melting temperature of 127°C. Since $LiNO_3$ is a relatively costly salt, therefore use of $LiNO_3$ in ternary blend increases the cost of ternary mixture. On the basis of above mentioned facts, the ternary mixture having composition of $LiNO_3$ (35 mol. %), $NaNO_3$ (17.5 mol. %) and KNO_3 (47.5 mol. %) has been studied theoretically and experimentally in the present work.

The melting point of ternary mixture determined from thermodynamic model is 124°C. In order to verify the melting point and to determine the thermal stability of novel ternary mixture, the DSC and TG analysis was carried out. The results obtained from DSC and TG analysis of novel ternary mixture are depicted in Figure 5.8. The melting point of ternary mixture determined from DSC is 121°C which is quite close to the value predicted by the thermodynamic model. The results obtained from TG shows that the ternary mixture is stable up to temperature of 534°C and can be used up to temperature of 608°C for short period.

Finally, the experimental results of ternary mixture of present study are compared with the previously reported experimental results of ternary mixture consisting of $LiNO_3$-$NaNO_3$-KNO_3 in Table 5.1. The results of present study as listed in Table 5.1 shows that the

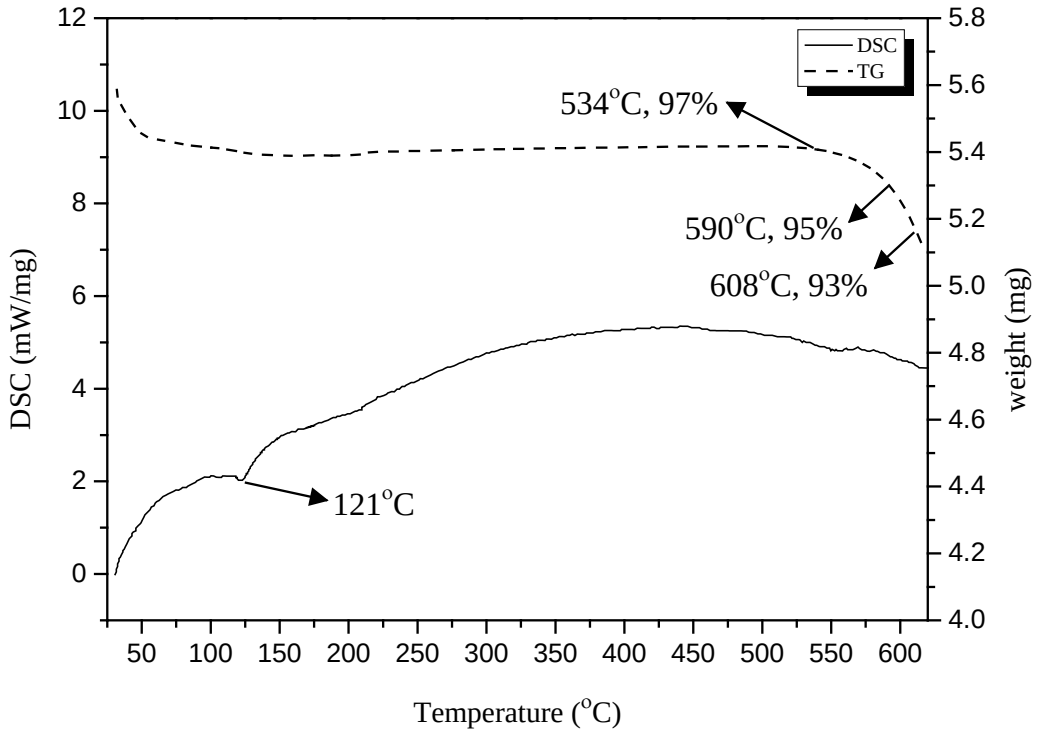

Figure 5.8: TG and DSC curves of ternary mixture of $LiNO_3$-$NaNO_3$-KNO_3.

eutectic composition and the melting temperature at eutectic composition of $LiNO_3$-$NaNO_3$-KNO_3 are in good agreement with the results of previous reported studies.

The reported eutectic mixture of $LiNO_3$ (30wt%), $NaNO_3$(17.8wt%) and KNO_3(52.2wt%) by Bergman and Nogoev has eutectic melting temperature of 120^0C. The reported eutectic temperature is slightly higher than eutectic melting temperature predicted from thermodynamic model due to higher concentration of $LiNO_3$ salt in reported ternary mixture. Moreover, the technique used to determine eutectic melting temperature was the visual polythermal method which was less accurate then DSC.

Table 5.1: Comparison of experimental results of previous and present study of ternary mixture consisting of $LiNO_3$-$NaNO_3$-KNO_3

		Wt.%		Temperature
Previous/present study	$LiNO_3$	$NaNO_3$	KNO3	°C
Bergman and Nogoev[30]	30	17.8	52.2	120
Reddy et al.[31]	25.92	20.01	54.02	117.6
Careth[32]	30	15	55	120
Present study	27.7	17.1	55.2	121

A novel eutectic composition of $LiNO_3$ (25.92 wt.%), $NaNO_3$(20.01 wt.%) and KNO_3(54.02wt%) using thermodynamic model was reported by Reddy et. al. the predicted eutectic melting temperature of 117^0C.

Careth reported a eutectic temperature of 120^0C at composition of $LiNO_3$(30wt%), $NaNO_3$(15wt%) and KNO_3(55wt%). The melting point reported by Careth was also slightly higher than our predicted temperature due to higher concentration of $LiNO_3$ in reported ternary mixture. The predicted eutectic melting point from thermodynamic model and experimentation are approximately equal and in good agreement with previous literature data.

Chapter 6

Conclusions and Future Scope of Work

6.1 Conclusions

1. Out of the three binary salt mixtures ($NaNO_3$-KNO_3, $LiNO_3$-$NaNO_3$ and $LiNO_3$-KNO_3) studied in this work, the binary mixture consisting of KNO_3 and $LiNO_3$ is found to be most suitable because the eutectic melting point of this binary mixture is determined to be 126.5 °C which is the lowest among all the three above mentioned binary mixtures. Moreover, this salt mixture is found to be thermally stable up to a temperature of 510 °C and can be used up to a temperature of 564 °C for a short period of time.
2. A ternary salt mixture consisting of $LiNO_3$-$NaNO_3$-KNO_3 is designed for solar thermal applications. The ternary salt has a eutectic composition of $LiNO_3$ (35 mol. %), $NaNO_3$ (17.5 mol. %) and KNO_3 (47.5 mol. %) and the melting point of this ternary mixture at eutectic composition is found to be 121°C. This salt mixture is thermally stable up to temperature of 534°C and can be used up to a temperature of 608°C for a short period of time. Moreover, this salt mixture is also cost effective due to lower concentration of lithium nitrate in the salt mixture.
3. The mathematical model based on regular solution theory has been used to predict the eutectic composition and melting point at the eutectic composition. It has been observed that the predicted results obtained from mathematical model are in good agreement with the results determined from experimental work. Therefore, it can be said the mathematical model based on regular solution theory has a good predictability and the same model can also be used to predict the results for a wide range of ternary and higher order systems.

6.2 Future Scope of Work

Further research into the thermodynamic models presented should include treating the salt's properties such as specific heat and latent heats, not as constants, but as functions of temperature. This may have the effect of improving the simulations. Another interesting analysis that could be conducted would be to investigate how changes in the binary coefficients would affect the ternary phase diagram simulations. For example, choosing

coefficients which may not produce an accurate binary simulation but will better match the ternary experimental data may be found. Conducting research into the possible effect of the addition of the ternary interaction between the three components, when modeling the ternary mixture should be done. This was assumed to be negligible in our models. The addition of other alkali metals should also be studied, such as rubidium or caesium. Alkaline nitrates could also be included in this research. Additionally, this thermodynamic model is not unique to nitrate systems, but could also be applied to other anion systems, for example halides. Use of these different compounds can provide further verification of the model. Lastly, using this formulation for higher-order systems, four or five components systems for instance should be investigated.

References

[1] Gomez, J., Glatzmaier, G. C., Starace, A., Turchi, C., and Ortega, J., 2011, “High Temperature Phase Change Materials for Thermal Energy Storage Applications Preprint,” (August), pp. 1-11.

[2] Kearney, D., Kelly, B., Cable, R., Potrovitza, N., Nava, P., Herrmann, U., Mahoney J. Pacheco, R., Price, H., and Blake, D., 2002, “Assessment of a Molten Salt Heat Transfer Fluid in a Parabolic Trough Solar Field,” Jsee, (April 2002), pp. 1–20.

[3] Fujiwara, M., Sano, T., Suzuki, K., and Watanabe, S., 1990, “Thermal Analysis and Fundamental Tests on a Heat Pipe Receiver for a Solar Dynamic Space Power System,” J. Sol. Energy Eng., **112**(3), p. 177.

[4] Kenisarin, M. M., 2010, “High-temperature phase change materials for thermal energy storage,” Renew. Sustain. Energy Rev., **14**(3), pp. 955–970.

[5] Shin BC, Kim SD, 1990, "Park WH., Ternary carbonate eutectic (lithium, sodium and potassium carbonates) for latent heat storage medium," Sol Energy Mater;21(1):81-90.

[6] Kamimoto, M., Tanaka, T., Tani, T., and Horigome, T., 1980, “Investigation of nitrate salts for solar latent heat storage,” Sol. Energy, **24**(6), pp. 581–587.

[7] Pacheco, J. E., 2002, “Final Test and Evaluation Results from the Solar Two Project,” Sandia Natl. Lab., (January), p. 294.

[8] Peng, Q., Yang, X. X., Ding, J., Wei, X. L., and Yang, J. P., 2013, “Design of new molten salt thermal energy storage material for solar thermal power plant,” Appl. Energy, **112**, pp. 682–689.

[9] Janz, G. J., Allen, Carolyn, B., Bansal, N. P., Murphy, R. M., and Tomkins, R. P. ., 1979, “Physical Properties Data Compilations Relevant to Energy Storage. II. Molten Salts: Data on Single and Multi-Components Salt Systems,” Natl. Bur. Stand.

[10] Bradshaw RW, Cordaro JG, Siegel NP.,2009, "Molten nitrate salt development for thermal energy storage in parabolic trough solar power systems," ASME Proc Energy Sustain, pp. 1–10.

[11] Cordaro J.G., Rubin N.C., Bradshaw R.W., 2011, “Multicomponent molten salt mixtures based on nitrate/nitrite anions,” Sol. Energy Eng., **133**(February), pp. 1–4.

[12] Raade, J. W., and Padowitz, D., 2010, “Development of molten salt Heat Transfer Fluid with low melting point and high thermal stability,” SolarPaces Conf., **1**(510), pp. 1–8.

[13] Vignarooban, K., Xu, X., Arvay, A., Hsu, K., and Kannan, A. M., 2015, “Heat transfer fluids for concentrating solar power systems – A review,” **146**, pp. 383–396.

[14] Zhai, W., Yang, B., Li, M., Li, S., Xin, M., Lin, J., and Wang, L., 2015, “Preparation of Multi nitrate molten salt and its properties tests,” (Ism3e), pp. 64–68.

[15] Rey, A., Lasanta, I., Mato, S., Brady, M. P., and Ferna, A. G., 2014, “Corrosion of alumina - forming austenitic steel in molten nitrate salts by gravimetric analysis and impedance spectroscopy,” (3), pp. 267–275.

[16] Fernández, A. G., Ushak, S., Galleguillos, H., and Pérez, F. J., 2014, “Development of new molten salts with $LiNO_3$ and $Ca(NO_3)_2$ for energy storage in CSP plants,” **119**(3), pp. 131–140.

[17] Chen, C., Olivares, R., and Wright, S., 2016, “Coupled Experimental Study and Thermodynamic Modeling of Melting Point and Thermal Stability of,” **136**(August 2014), pp. 1–7.

[18] Kuravi, S., Goswami, Y., Stefanakos, E. K., Ram, M., Jotshi, C., Pendyala, S., Trahan, J., Sridharan, P., Rahman, M., and Krakow, B., 2012, “Thermal Energy Storage For Concentrating Solar Power Plants,” **14**, pp. 81–91.

[19] Zhao, C. Y., and Wu, Z. G., 2011, “Solar Energy Materials & Solar Cells Thermal property characterization of a low melting-temperature ternary nitrate salt mixture for thermal energy storage systems,” **95**, pp. 3341–3346.

[20] Wang, T., Mantha, D., and Reddy, R. G., 2015, “Solar Energy Materials & Solar Cells Novel high thermal stability LiF – Na_2CO_3 – K_2CO_3 eutectic ternary system for thermal energy storage applications,” **140**, pp. 366–375.

[21] Coscia, K., and Elliott, T., 2015, “Binary and Ternary Nitrate Solar Heat Transfer Fluids,” Trans. ASME, **135**(May 2013), pp. 1–6.

[22] Kramer, C. M., and Wilson, C. J., 1980, “The phase diagram of $NaNO_3$-KNO_3 ,” **42**(3), pp. 253–264.

[23] Zhang, X., Xu, K., and Gao, Y., 2002, “The phase diagram of $LiNO_3$ – KNO_3,” **385**(July 2001), pp. 81–84.

[24] Zhang, X., Tian, J., Xu, K., and Gao, Y., 2003, “Thermodynamic evaluation of phase equilibria in NaNO3-KNO3 system,” J. phase equilibria, **24**(5), pp. 441–446.

[25] Vallet, C., 1972, “Phase diagrams and thermodynamic properties of some molten nitrate mixtures,” J. Chem. Thermodyn., **4**(1), pp. 105–114.

[26] Wu, Y., Liu, S., Xiong, Y., Ma, C., and Ding, Y., 2015, “Experimental study on the heat transfer characteristics of a low melting point salt in a parabolic trough solar collector system,” **89**, pp. 748–754.

[27] Bale, C. W., and Pelton, A. D., 1997, “The Unified Interaction Parameter Formalism " Thermodynamic Consistency and Applications,” **21**(July 1990).

[28] Kleppa, O. J., and Hersh, L. S., 1961, “Heats of Mixing in Liquid Alkali Nitrate Systems,” J. Chem. Phys., **34**(2), p. 351.

[29] Campbell, A. N., Kartzmark, E. M., and Nagarajan, M. K., 1962, “The binary (anhydrous) systems $NaNO_3$-$LiNO_3$, $LiClO_3$-$NaClO_3$, $LiClO_3$-$LiNO_3$, $NaNO_3$-$NaClO_3$ and the quaternary system $NaNO_3$-$LiNO_3$- $LiClO_3$-$NaClO_3$,” Can. J. Biochem., 40(7), pp. 1258–1265.

[30] Bergman, A. G., and Nogoev, K., 1964, “The $CO(NH_2)_2$-$LiNO_3$; K, Li, Na || NO_3; and K, NH_4, Na || NO_3 Systems,” Russ. J. Inorg. Chem., 9(6), pp. 771–773.

[31] Reddy, R.G., 2010, “Novel Molten Salts Thermal Energy Storage for Concentrating Solar Power Generation,” U.S. Department of Energy, Solar Energy Technologies ProgramPeer,Review,availableat:http://www1.eere.energy.gov/solar/review_meeting/pdfs/prm2010_exec_summary.pdf

[32] Mellor, J. W., 1922, A Comprehensive Treatise On Inorganic and Theoretical Chemistry, Longmans, Green and Co., New York, Vol. 2.

Appendix A: MATLAB Scripts

```
%%%%%%%%%%%%%%%%%%%%%%%%%%%%%%%%%%%%%%%%%%%%%%%%%%%%%%%%%%%%%%%%%%%%%%%%%%%%

% Script to obtain phase diagram of of NaNO3-LiNO3 binary salt system

% Written by Abhishek Upadhyay 2016

%%%%%%%%%%%%%%%%%%%%%%%%%%%%%%%%%%%%%%%%%%%%%%%%%%%%%%%%%%%%%%%%%%%%%%%%%%%%

clear all
clc
%Set individual melting temperature for salts A and B
Tm1=577.5;
Tm2=607.4;
%Set latent heat of fusion for salts A and B
H1=14704.0831;
H2=9766.5498;
%Set value of change in specific heat for salts A and B
C1=-9.3494;
C2=-3.03309;
%Set value of empirical coefficient of salts A and B
as=6276;
bs=0;
cs=0;
al=-1707;
bl=-284.5;
cl=0;
R=8.3144621;
%xbl=0.1;
%Set mole fractions for component B
xbl=0.01:0.01:0.99;
n=length(xbl);
%Set initial guess
x=[0.99;0.99;0.01;570];
for i=1:n
%Set options for fsolve
options=optimset('MaxIter',50000,'MaxFunEvals',75000,'TolFun',1.0e-
16,'TolX',1.0e-16,'Display','iter');
%Optimize
[x,fval]=fsolve(@eqn,x,options,R,cl,bl,al,cs,bs,as,C1,C2,H1,H2,Tm1,T
m2,xbl(i))
X(i,1)=x(1);
X(i,2)=x(2);
```

```
X(i,3)=x(3);
X(i,4)=x(4);
plot(xbl(i),x(4),'b',x(3),x(4),'k'); hold on; grid on;
end


%%%%%%%%%%%%%%%%%%%%%%%%%%%%%%%%%%%%%%%%%%%%%%%%%%%%%%%%%%%%%%%%%%%%%%%%%%%%

% First part of Script to obtain phase diagram of of LiNO3-NaNO3 binary
salt system

% Written by Abhishek Upadhyay 2016

%%%%%%%%%%%%%%%%%%%%%%%%%%%%%%%%%%%%%%%%%%%%%%%%%%%%%%%%%%%%%%%%%%%%%%%%%%%%

clear all
clc
%Set individual melting temperature for salts A and B
Tm1=525.9;
Tm2=577.5;
%Set latent heat of fusion for salts A and B
H1=25027.398;
H2=14704.0831;
%Set value of change in specific heat for salts A and B
C1=17.2365;
C2=-9.3494;
%Set value of empirical coefficient of salts A and B
as=9204.8;
bs=3347.2;
cs=0;
al=-1941.4;
bl=-2928.8;
cl=0;
R=8.3144621;
%xbl=0.01;
%Set mole fractions for component B
xbl=0.99:-0.01:0.40;
n=length(xbl);
%Set initial guess
x=[0.01;0.01;0.99;578];
for i=1:n
%Set options for fsolve

options=optimset('MaxIter',50000,'MaxFunEvals',75000,'TolFun',1.0e-
16,'TolX',1.0e-16,'Display','iter');
```

```
%Optimize
[x,fval]=fsolve(@eqn,x,options,R,cl,bl,al,cs,bs,as,C1,C2,H1,H2,Tm1,T
m2,xbl(i))
X(i,1)=x(1);
X(i,2)=x(2);
X(i,3)=x(3);
X(i,4)=x(4);
plot(xbl(i),x(4),'b',x(3),x(4),'k'); hold on; grid on;
end


%%%%%%%%%%%%%%%%%%%%%%%%%%%%%%%%%%%%%%%%%%%%%%%%%%%%%%%%%%%%%%%%%%%%%%%%%%%%

% Second part of Script to obtain phase diagram of of LiNO3-NaNO3
binary salt system

% Written by Abhishek Upadhyay 2016

%%%%%%%%%%%%%%%%%%%%%%%%%%%%%%%%%%%%%%%%%%%%%%%%%%%%%%%%%%%%%%%%%%%%%%%%%%%%

clear all
clc
%Set individual melting temperature for salts A and B
Tm1=525.9;
Tm2=577.5;
%Set latent heat of fusion for salts A and B
H1=25027.398;
H2=14704.0831;
%Set value of change in specific heat for salts A and B
C1=17.2365;
C2=-9.3494;
%Set value of empirical coefficient of salts A and B
as=9204.8;
bs=3347.2;
cs=0;
al=-1941.4;
bl=-2928.8;
cl=0;
R=8.3144621;
%xbl=0.01;
%Set mole fractions for component B
xbl=0.01:0.01:0.60;
n=length(xbl);
%Set initial guess
x=[0.99;0.99;0.01;526];
```

```
for i=1:n
%Set options for fsolve
options=optimset('MaxIter',50000,'MaxFunEvals',75000,'TolFun',1.0e-16,'TolX',1.0e-16,'Display','iter');
%Optimize
[x,fval]=fsolve(@eqn,x,options,R,cl,bl,al,cs,bs,as,C1,C2,H1,H2,Tm1,Tm2,xbl(i))
X(i,1)=x(1);
X(i,2)=x(2);
X(i,3)=x(3);
X(i,4)=x(4);
plot(xbl(i),x(4),'b',x(3),x(4),'k'); hold on; grid on;
end

%%%%%%%%%%%%%%%%%%%%%%%%%%%%%%%%%%%%%%%%%%%%%%%%%%%%%%%%%%%%%%%%%%%%%%%%%%%%%%%%%%

% First part of Script to obtain phase diagram of of LiNO3-KNO3 binary salt system

% Written by Abhishek Upadhyay 2016

%%%%%%%%%%%%%%%%%%%%%%%%%%%%%%%%%%%%%%%%%%%%%%%%%%%%%%%%%%%%%%%%%%%%%%%%%%%%%%%%%%

clear all
clc
%Set individual melting temperature for salts A and B
Tm1=525.9;
Tm2=607.4;
%Set latent heat of fusion for salts A and B
H1=25027.398;
H2=9766.5498;
%Set value of change in specific heat for salts A and B
C1=17.2365;
C2=-3.03309;
%Set value of empirical coefficient of salts A and B
as=10460;
bs=4184;
cs=0;
al=-9183.9;
bl=-364;
cl=-1937.2;
R=8.3144621;
%xbl=0.01;
%Set mole fractions for component B
```

```
xbl=0.55:0.01:0.99;
n=length(xbl);
%Set initial guess
x=[0.01;0.01;0.99;608];
for i=1:n
%Set options for fsolve
options=optimset('MaxIter',50000,'MaxFunEvals',75000,'TolFun',1.0e-
16,'TolX',1.0e-16,'Display','iter');
%Optimize
[x,fval]=fsolve(@eqn,x,options,R,cl,bl,al,cs,bs,as,C1,C2,H1,H2,Tm1,T
m2,xbl(i))
X(i,1)=x(1);
X(i,2)=x(2);
X(i,3)=x(3);
X(i,4)=x(4);
plot(xbl(i),x(4),'b',x(3),x(4),'k'); hold on; grid on;
end
```

```
%%%%%%%%%%%%%%%%%%%%%%%%%%%%%%%%%%%%%%%%%%%%%%%%%%%%%%%%%%%%%%%%%%%%%%%%%%%%%%%
```

% Second part of Script to obtain phase diagram of of $LiNO_3$-KNO_3 binary salt system

% Written by Abhishek Upadhyay 2016

```
%%%%%%%%%%%%%%%%%%%%%%%%%%%%%%%%%%%%%%%%%%%%%%%%%%%%%%%%%%%%%%%%%%%%%%%%%%%%%%%
```

```
clear all
clc
%Set individual melting temperature for salts A and B
Tm1=525.9;
Tm2=607.4;
%Set latent heat of fusion for salts A and B
H1=25027.398;
H2=9766.5498;
%Set value of change in specific heat for salts A and B
C1=17.2365;
C2=-3.03309;
%Set value of empirical coefficient of salts A and B
as=10460;
bs=4184;
cs=0;
al=-9183.9;
```

```
bl=-364;
cl=-1937.2;
R=8.3144621;
%xbl=0.01;
%Set mole fractions for component B
xbl=0.01:0.01:0.65;
n=length(xbl);
%Set initial guess
x=[0.99;0.99;0.01;526];
for i=1:n
%Set options for fsolve
options=optimset('MaxIter',50000,'MaxFunEvals',75000,'TolFun',1.0e-
16,'TolX',1.0e-16,'Display','iter');
%Optimize
[x,fval]=fsolve(@eqn,x,options,R,cl,bl,al,cs,bs,as,C1,C2,H1,H2,Tm1,T
m2,xbl(i))
X(i,1)=x(1);
X(i,2)=x(2);
X(i,3)=x(3);
X(i,4)=x(4);
plot(xbl(i),x(4),'b',x(3),x(4),'k'); hold on; grid on;
end


%%%%%%%%%%%%%%%%%%%%%%%%%%%%%%%%%%%%%%%%%%%%%%%%%%%%%%%%%%%%%%%%%%%%%%%%%%%

% Script of Binary equation

% Written by Abhishek Upadhyay 2016

%%%%%%%%%%%%%%%%%%%%%%%%%%%%%%%%%%%%%%%%%%%%%%%%%%%%%%%%%%%%%%%%%%%%%%%%%%%


function F = eqn(x,R,cl,bl,al,cs,bs,as,C1,C2,H1,H2,Tm1,Tm2,xbl)
F=[(1-x(4)/Tm1)*H1+C1*(x(4)-Tm1-
x(4)*log(x(4)/Tm1))+R*x(4)*(log(x(1))-
log(x(2)))+(al*xbl^2+2*bl*x(1)*xbl^2+2*cl*x(1)*xbl^3-
cl*x(1)^2*xbl^2)+(x(2)^2*x(3)^2*cs-2*x(2)*x(3)^3*cs-
2*x(2)*x(3)^2*bs-x(3)^2*as);(1-x(4)/Tm2)*H2+C2*(x(4)-Tm2-
x(4)*log(x(4)/Tm2))+R*x(4)*(log(xbl)-
log(x(3)))+(al*x(1)^2+bl*x(1)^3-bl*x(1)^2*xbl+2*cl*x(1)^3*xbl-
cl*x(1)^2*xbl^2)-(2*x(2)^3*x(3)*cs-x(2)^2*x(3)^2*cs+x(2)^3*bs-
x(2)^2*x(3)*bs+x(2)^2*as);x(1)+xbl-1;x(2)+x(3)-1];
```

```
%%%%%%%%%%%%%%%%%%%%%%%%%%%%%%%%%%%%%%%%%%%%%%%%%%%%%%%%%%%%%%%%%%%%%%%%%%%%

% Script to obtain phase diagram of of LiNO3-NaNO3-KNO3 binary salt
system

% Written by Abhishek Upadhyay 2016

%%%%%%%%%%%%%%%%%%%%%%%%%%%%%%%%%%%%%%%%%%%%%%%%%%%%%%%%%%%%%%%%%%%%%%%%%%%%

clear all
clc
%Set individual melting temperature for salts A and B
T1=525.9;
T2=607.4;
T3=577.5;
%Set latent heat of fusion for salts A and B
H1=25027.398;
H2=9766.5498;
H3=14704.0831;
%Set value of change in specific heat for salts A and B
C1=17.2365;
C2=-3.03309;
C3=-9.3494;
%Set value of empirical coefficient of salts A and B
as3=9204.8;
bs3=3347.2;
cs3=0;
al3=-1941.4;
bl3=-2928.8;
cl3=0;
al1=-9183.9;
bl1=-364;
cl1=-1937.2;
as1=10460;
bs1=4184;
cs1=0;
al2=-1707;
bl2=-284.5;
cl2=0;
as2=6276;
bs2=0;
cs2=0;
R=8.3144621;
%Set mole fractions for component A
```

```
xal=0.1:0.05:0.40;
m=length(xal);
for j=1:m
%Set mole fractions for component B
    xbl=0.01:0.01:(0.99-xal(j));
    n=length(xbl);
%Set initial guess
    x=[0.89;0.1;0.01;0.95;563];
for i=1:n
%Set options for fsolve
options=optimset('MaxIter',50000,'MaxFunEvals',75000,'TolFun',1.0e-
16,'TolX',1.0e-16,'Display','iter');
%Optimize
[x,fval]=fsolve(@eqnternary,x,options,R,T1,T2,T3,C1,C2,C3,H1,H2,H3,a
l1,bl1,as1,al2,bl2,cl2,as2,bs2,al3,bl3,as3,bs3,xal(j),xbl(i))
X(j,i,1)=x(1);
X(j,i,2)=x(2);
X(j,i,3)=x(3);
X(j,i,4)=x(4);
X(j,i,5)=x(5);
plot(xbl(i),x(5),'b'); hold on; grid on;
end
end
```

```
%%%%%%%%%%%%%%%%%%%%%%%%%%%%%%%%%%%%%%%%%%%%%%%%%%%%%%%%%%%%%%%%%%%%%%%%%%%%

% Script of Ternary equation

% Written by Abhishek Upadhyay 2016

%%%%%%%%%%%%%%%%%%%%%%%%%%%%%%%%%%%%%%%%%%%%%%%%%%%%%%%%%%%%%%%%%%%%%%%%%%%%


functionF=eqnternary(x,R,T1,T2,T3,C1,C2,C3,H1,H2,H3,al1,bl1,as1,al2,
bl2,cl2,as2,bs2,al3,bl3,as3,bs3,xal,xbl)
F=[(1-(x(5)/T1))*H1+C1*(x(5)-T1-
x(5)*(log((x(5))/T1)))+R*x(5)*(log(xal)-log(x(2)))+((1-
xal)*(al1*xbl+2*bl1*xal*xbl+al3*x(1)+bl3*(x(1))^2)-al2*xbl*x(1)-
2*bl2*xbl*(x(1))^2-bl3*xal*(x(1))^2-3*cl2*xbl^2*(x(1))^2)-((1-
x(2))*(as1*x(3)+as3*x(4)+bs3*(x(4))^2)-as2*x(3)*x(4)-
2*bs2*x(3)*(x(4))^2-bs3*x(2)*(x(4))^2);xal+xbl+x(1)-
1;x(2)+x(3)+x(4)-1;(1-(x(5)/T2))*H2+C2*(x(5)-T2-
x(5)*(log((x(5))/T2)))+R*x(5)*(log(xbl)-log(x(3)))+((1-
xbl)*(al1*xal+bl1*xal^2+al2*x(1)+bl2*(x(1))^2+2*cl2*xbl*(x(1))^2)-
bl1*xal^2*xbl-bl2*xbl*(x(1))^2-cl2*xbl^2*(x(1))^2-
2*bl3*xal*(x(1))^2-al3*xal*x(1))-((1-
x(3))*(as1*x(2)+as2*x(4)+bs2*(x(4))^2)-bs2*x(3)*(x(4))^2-
as3*x(2)*x(4)-2*bs3*x(2)*(x(4))^2);(1-(x(5)/T3))*H3+C3*(x(5)-T3-
x(5)*(log((x(5))/T3)))+R*x(5)*(log(x(1))-log(x(4)))+((1-
x(1))*(al2*xbl+2*bl2*xbl*x(1)+2*cl2*xbl^2*x(1)+al3*xal+2*bl3*xal*x(1
))-al1*xal*xbl-2*bl1*xal^2*xbl-cl2*xbl^2*(x(1))^2)-((1-
x(4))*(as2*x(3)+2*bs2*x(3)*x(4)+as3*x(2)+2*bs3*x(2)*x(4))-
as1*x(2)*x(3))];
```

Appendix B: Simulation Results

Table B1: Solidus temperature of $NaNO_3$-KNO_3 binary mixture from thermodynamic model.

X_{BS}	T(°C)	X_{BS}	T(°C)
0.002008	302.8285	0.435185	220.7896
0.004079	301.2903	0.484395	220.3786
0.006216	299.7357	0.536052	220.3351
0.008421	298.1649	0.585543	220.6785
0.010697	296.5784	0.629638	221.3875
0.013047	294.9763	0.6675	222.4162
0.015473	293.3591	0.699692	223.7137
0.01798	291.7269	0.727164	225.2342
0.02057	290.0801	0.750817	226.9394
0.023247	288.419	0.77139	228.7982
0.026015	286.744	0.789462	230.7855
0.028879	285.0554	0.805482	232.881
0.031842	283.3536	0.819797	235.0682
0.034911	281.6389	0.832683	237.3333
0.038091	279.9117	0.844354	239.665
0.041387	278.1724	0.854987	242.0538
0.044807	276.4214	0.864721	244.4917
0.048356	274.6592	0.873675	246.9717
0.052044	272.8862	0.881943	249.488
0.055878	271.1029	0.889606	252.0354
0.059868	269.3098	0.896733	254.6096
0.064024	267.5076	0.903381	257.2068
0.068357	265.6967	0.9096	259.8235
0.072881	263.8779	0.915432	262.4567
0.077609	262.0518	0.920915	265.1038
0.082557	260.2193	0.926081	267.7624
0.087743	258.3811	0.930957	270.4304
0.093186	256.5382	0.935569	273.1061
0.09891	254.6916	0.93994	275.7876
0.104938	252.8424	0.944088	278.4734
0.111302	250.992	0.948031	281.1622
0.118033	249.1417	0.951785	283.8528
0.125172	247.2933	0.955363	286.5439
0.132762	245.4485	0.958779	289.2347
0.140857	243.6095	0.962044	291.9241
0.149518	241.7788	0.965168	294.6112
0.158819	239.9593	0.968161	297.2954
0.16885	238.1544	0.971031	299.9759
0.179718	236.3681	0.973786	302.6521
0.191554	234.6053	0.976434	305.3233
0.204523	232.8719	0.97898	307.9889
0.21883	231.1751	0.981431	310.6486

0.234736	229.5239	0.983792	313.3019
0.25258	227.9296	0.986069	315.9482
0.272801	226.4068	0.988267	318.5872
0.295977	224.9744	0.990388	321.2186
0.322861	223.6574	0.992439	323.842
0.354395	222.4893	0.994422	326.4571
0.39161	221.5145	0.996341	329.0636

Table B2: Liquidus temperature of $NaNO_3$-KNO_3 binary mixture from thermodynamic model.

X_{BL}	T(°C)	X_{BL}	T(°C)
0.01	302.8285	0.5	220.7896
0.02	301.2903	0.51	220.3786
0.03	299.7357	0.52	220.3351
0.04	298.1649	0.53	220.6785
0.05	296.5784	0.54	221.3875
0.06	294.9763	0.55	222.4162
0.07	293.3591	0.56	223.7137
0.08	291.7269	0.57	225.2342
0.09	290.0801	0.58	226.9394
0.1	288.419	0.59	228.7982
0.11	286.744	0.6	230.7855
0.12	285.0554	0.61	232.881
0.13	283.3536	0.62	235.0682
0.14	281.6389	0.63	237.3333
0.15	279.9117	0.64	239.665
0.16	278.1724	0.65	242.0538
0.17	276.4214	0.66	244.4917
0.18	274.6592	0.67	246.9717
0.19	272.8862	0.68	249.488
0.2	271.1029	0.69	252.0354
0.21	269.3098	0.7	254.6096
0.22	267.5076	0.71	257.2068
0.23	265.6967	0.72	259.8235
0.24	263.8779	0.73	262.4567
0.25	262.0518	0.74	265.1038
0.26	260.2193	0.75	267.7624
0.27	258.3811	0.76	270.4304
0.28	256.5382	0.77	273.1061
0.29	254.6916	0.78	275.7876
0.3	252.8424	0.79	278.4734
0.31	250.992	0.8	281.1622
0.32	249.1417	0.81	283.8528
0.33	247.2933	0.82	286.5439
0.34	245.4485	0.83	289.2347
0.35	243.6095	0.84	291.9241
0.36	241.7788	0.85	294.6112

0.37	239.9593	0.86	297.2954
0.38	238.1544	0.87	299.9759
0.39	236.3681	0.88	302.6521
0.4	234.6053	0.89	305.3233
0.41	232.8719	0.9	307.9889
0.42	231.1751	0.91	310.6486
0.43	229.5239	0.92	313.3019
0.44	227.9296	0.93	315.9482
0.45	226.4068	0.94	318.5872
0.46	224.9744	0.95	321.2186
0.47	223.6574	0.96	323.842
0.48	222.4893	0.97	326.4571
0.49	221.5145	0.98	329.0636

Table B3: Solidus temperature of $LiNO_3$-KNO_3 binary mixture from thermodynamic model.

X_{BS}	T(°C)	X_{BS}	T(°C)
5.52947E-5	251.81607	0.01022	145.7879
1.14105E-4	250.84149	0.01062	142.27983
1.76596E-4	249.82542	0.01103	138.71713
2.42933E-4	248.76706	0.01144	135.09986
3.13285E-4	247.66563	0.01186	131.42812
3.87825E-4	246.52038	0.01228	127.70195
4.66726E-4	245.3306	0.0127	123.92142
5.50165E-4	244.09559	0.95378	126.05888
6.38319E-4	242.81469	0.9591	132.05578
7.31367E-4	241.48725	0.96366	138.06203
8.2949E-4	240.11267	0.96759	144.06647
9.3287E-4	238.69036	0.97101	150.05969
0.00104	237.21976	0.974	156.03362
0.00116	235.70033	0.97663	161.9812
0.00128	234.13157	0.97895	167.89623
0.0014	232.51298	0.98101	173.77316
0.00153	230.84411	0.98285	179.60699
0.00167	229.12452	0.98449	185.39318
0.00182	227.35379	0.98595	191.12761
0.00197	225.53153	0.98727	196.8065
0.00213	223.65737	0.98846	202.42635
0.0023	221.73097	0.98953	207.98395
0.00247	219.75199	0.9905	213.47633
0.00265	217.72015	0.99138	218.90076
0.00284	215.63515	0.99217	224.25468
0.00303	213.49673	0.9929	229.53574
0.00324	211.30465	0.99356	234.74178
0.00345	209.0587	0.99416	239.8708
0.00367	206.75866	0.99471	244.92097
0.00389	204.40436	0.99521	249.8906

0.00413	201.99563	0.99567	254.77819
0.00437	199.53233	0.99609	259.58236
0.00463	197.01432	0.99647	264.30188
0.00489	194.4415	0.99683	268.93569
0.00516	191.81377	0.99715	273.48284
0.00544	189.13104	0.99745	277.94254
0.00572	186.39327	0.99773	282.31416
0.00602	183.6004	0.99799	286.59719
0.00632	180.75239	0.99822	290.79126
0.00664	177.84922	0.99844	294.89617
0.00696	174.8909	0.99864	298.91183
0.00729	171.87742	0.99883	302.83832
0.00763	168.80879	0.999	306.67587
0.00798	165.68506	0.99916	310.42483
0.00833	162.50625	0.99931	314.08573
0.0087	159.2724	0.99944	317.65923
0.00907	155.98358	0.99957	321.14616
0.00945	152.63985	0.99969	324.54749
0.00983	149.24126	0.9998	327.86435

Table B4: Liquidus temperature of $LiNO_3$-KNO_3 binary mixture from thermodynamic model.

X_{BL}	T(°C)	X_{BL}	T(°C)
0.01	251.81607	0.5	145.7879
0.02	250.84149	0.51	142.27983
0.03	249.82542	0.52	138.71713
0.04	248.76706	0.53	135.09986
0.05	247.66563	0.54	131.42812
0.06	246.52038	0.55	127.70195
0.07	245.3306	0.56	123.92142
0.08	244.09559	0.57	126.05888
0.09	242.81469	0.58	132.05578
0.1	241.48725	0.59	138.06203
0.11	240.11267	0.6	144.06647
0.12	238.69036	0.61	150.05969
0.13	237.21976	0.62	156.03362
0.14	235.70033	0.63	161.9812
0.15	234.13157	0.64	167.89623
0.16	232.51298	0.65	173.77316
0.17	230.84411	0.66	179.60699
0.18	229.12452	0.67	185.39318
0.19	227.35379	0.68	191.12761
0.2	225.53153	0.69	196.8065
0.21	223.65737	0.7	202.42635
0.22	221.73097	0.71	207.98395
0.23	219.75199	0.72	213.47633
0.24	217.72015	0.73	218.90076

0.25	215.63515	0.74	224.25468
0.26	213.49673	0.75	229.53574
0.27	211.30465	0.76	234.74178
0.28	209.0587	0.77	239.8708
0.29	206.75866	0.78	244.92097
0.3	204.40436	0.79	249.8906
0.31	201.99563	0.8	254.77819
0.32	199.53233	0.81	259.58236
0.33	197.01432	0.82	264.30188
0.34	194.4415	0.83	268.93569
0.35	191.81377	0.84	273.48284
0.36	189.13104	0.85	277.94254
0.37	186.39327	0.86	282.31416
0.38	183.6004	0.87	286.59719
0.39	180.75239	0.88	290.79126
0.4	177.84922	0.89	294.89617
0.41	174.8909	0.9	298.91183
0.42	171.87742	0.91	302.83832
0.43	168.80879	0.92	306.67587
0.44	165.68506	0.93	310.42483
0.45	162.50625	0.94	314.08573
0.46	159.2724	0.95	317.65923
0.47	155.98358	0.96	321.14616
0.48	152.63985	0.97	324.54749
0.49	149.24126	0.98	327.86435

Table B5: Solidus temperature of $LiNO_3$-$NaNO_3$ binary mixture from thermodynamic model.

X_{BL}	T(°C)	X_{BL}	T(°C)
2.61868E-4	251.83562	0.90974	195.61649
5.42858E-4	250.88419	0.91592	198.44831
8.43597E-4	249.89648	0.9215	201.25767
0.00116	248.87321	0.92657	204.04207
0.00151	247.81513	0.9312	206.79951
0.00187	246.72296	0.93544	209.5284
0.00226	245.59743	0.93934	212.22751
0.00267	244.43925	0.94294	214.89586
0.0031	243.24911	0.94628	217.53272
0.00356	242.02773	0.94938	220.13753
0.00404	240.77577	0.95227	222.70994
0.00455	239.49394	0.95497	225.24969
0.00509	238.18289	0.95749	227.7567
0.00565	236.8433	0.95986	230.23097
0.00624	235.47583	0.96208	232.6726
0.00687	234.08111	0.96417	235.08179
0.00752	232.6598	0.96614	237.45882
0.0082	231.21252	0.968	239.80403

0.00892	229.7399	0.96976	242.11783
0.00967	228.24257	0.97143	244.4007
0.01046	226.72112	0.97301	246.65318
0.01128	225.17616	0.97451	248.87584
0.01215	223.60829	0.97594	251.06931
0.01305	222.01808	0.9773	253.23428
0.01399	220.40612	0.9786	255.37147
0.01498	218.77297	0.97984	257.48164
0.01601	217.11919	0.98103	259.56558
0.01709	215.44534	0.98216	261.62414
0.01822	213.75195	0.98325	263.65819
0.0194	212.03956	0.98429	265.66864
0.02064	210.3087	0.9853	267.65642
0.02194	208.55988	0.98626	269.62252
0.0233	206.79361	0.98719	271.56792
0.02472	205.0104	0.98809	273.49366
0.02622	203.21073	0.98896	275.40079
0.02779	201.3951	0.98979	277.29042
0.02944	199.56399	0.9906	279.16364
0.03118	197.71786	0.99139	281.0216
0.03302	195.85719	0.99215	282.86546
0.03496	193.98245	0.99289	284.69642
0.03702	192.09409	0.99361	286.51569
0.03921	190.19259	0.99432	288.32452
0.04153	188.27842	0.995	290.12416
0.04402	186.35205	0.99567	291.9159
0.04669	184.41398	0.99633	293.70106
0.87613	184.14308	0.99697	295.48097
0.88628	187.02266	0.99759	297.25698
0.8951	189.89904	0.99821	299.03048
0.90285	192.76539	0.99882	300.80286

Table B6: Liquidus temperature of $LiNO_3$-$NaNO_3$ binary mixture from thermodynamic model.

X_{BL}	T(°C)	X_{BL}	T(°C)
0.01	251.83562	0.5	195.61649
0.02	250.88419	0.51	198.44831
0.03	249.89648	0.52	201.25767
0.04	248.87321	0.53	204.04207
0.05	247.81513	0.54	206.79951
0.06	246.72296	0.55	209.5284
0.07	245.59743	0.56	212.22751
0.08	244.43925	0.57	214.89586
0.09	243.24911	0.58	217.53272
0.1	242.02773	0.59	220.13753
0.11	240.77577	0.6	222.70994
0.12	239.49394	0.61	225.24969

0.13	238.18289	0.62	227.7567
0.14	236.8433	0.63	230.23097
0.15	235.47583	0.64	232.6726
0.16	234.08111	0.65	235.08179
0.17	232.6598	0.66	237.45882
0.18	231.21252	0.67	239.80403
0.19	229.7399	0.68	242.11783
0.2	228.24257	0.69	244.4007
0.21	226.72112	0.7	246.65318
0.22	225.17616	0.71	248.87584
0.23	223.60829	0.72	251.06931
0.24	222.01808	0.73	253.23428
0.25	220.40612	0.74	255.37147
0.26	218.77297	0.75	257.48164
0.27	217.11919	0.76	259.56558
0.28	215.44534	0.77	261.62414
0.29	213.75195	0.78	263.65819
0.3	212.03956	0.79	265.66864
0.31	210.3087	0.8	267.65642
0.32	208.55988	0.81	269.62252
0.33	206.79361	0.82	271.56792
0.34	205.0104	0.83	273.49366
0.35	203.21073	0.84	275.40079
0.36	201.3951	0.85	277.29042
0.37	199.56399	0.86	279.16364
0.38	197.71786	0.87	281.0216
0.39	195.85719	0.88	282.86546
0.4	193.98245	0.89	284.69642
0.41	192.09409	0.9	286.51569
0.42	190.19259	0.91	288.32452
0.43	188.27842	0.92	290.12416
0.44	186.35205	0.93	291.9159
0.45	184.41398	0.94	293.70106
0.46	184.14308	0.95	295.48097
0.47	187.02266	0.96	297.25698
0.48	189.89904	0.97	299.03048
0.49	192.76539	0.98	300.80286

Table B7: Liquidus temperature of $LiNO_3$-$NaNO_3$- KNO_3 ternary mixture from thermodynamic model at fixed concentration of $LiNO_3$ at 2%.

X_{BL}	T(°C)	X_{BL}	T(°C)
0.01	298.97535	0.5	216.87293
0.02	297.42142	0.51	216.57238
0.03	295.85181	0.52	216.66283
0.04	294.26681	0.53	217.14761
0.05	292.66667	0.54	217.99034

0.06	291.05168	0.55	219.13813
0.07	289.42212	0.56	220.53907
0.08	287.77827	0.57	222.14881
0.09	286.12043	0.58	223.93131
0.1	284.4489	0.59	225.85764
0.11	282.76399	0.6	227.90457
0.12	281.06601	0.61	230.05332
0.13	279.3553	0.62	232.28855
0.14	277.63219	0.63	234.5976
0.15	275.89706	0.64	236.96996
0.16	274.15025	0.65	239.39678
0.17	272.39218	0.66	241.87058
0.18	270.62325	0.67	244.38497
0.19	268.8439	0.68	246.93447
0.2	267.05459	0.69	249.51433
0.21	265.25582	0.7	252.12043
0.22	263.44813	0.71	254.74917
0.23	261.63208	0.72	257.39737
0.24	259.80829	0.73	260.06226
0.25	257.97745	0.74	262.74136
0.26	256.1403	0.75	265.43246
0.27	254.29765	0.76	268.1336
0.28	252.4504	0.77	270.84304
0.29	250.59955	0.78	273.55919
0.3	248.74624	0.79	276.28063
0.31	246.89171	0.8	279.00609
0.32	245.03741	0.81	281.73441
0.33	243.18495	0.82	284.46454
0.34	241.33621	0.83	287.19553
0.35	239.49333	0.84	289.92652
0.36	237.65885	0.85	292.65671
0.37	235.83569	0.86	295.3854
0.38	234.02735	0.87	298.11192
0.39	232.238	0.88	300.83568
0.4	230.47267	0.89	303.55614
0.41	228.73752	0.9	306.27278
0.42	227.04017	0.91	308.98517
0.43	225.39016	0.92	311.69286
0.44	223.79968	0.93	314.3955
0.45	222.28454	0.94	317.09271
0.46	220.86557	0.95	319.78419
0.47	219.57072	0.96	322.46964
0.48	218.43776	0.97	325.14879
0.49	217.51727		

Table B8: Liquidus temperature of $LiNO_3$-$NaNO_3$- KNO_3 ternary mixture from thermodynamic model at fixed concentration of $LiNO_3$ at 10%.

X_{BL}	T(°C)	X_{BL}	T(°C)
0.01	281.38087	0.5	199.65444
0.02	279.79804	0.51	199.85355
0.03	278.2018	0.52	200.48865
0.04	276.59235	0.53	201.49478
0.05	274.96984	0.54	202.80299
0.06	273.33447	0.55	204.3554
0.07	271.68642	0.56	206.10665
0.08	270.02586	0.57	208.02163
0.09	268.353	0.58	210.07295
0.1	266.66802	0.59	212.23904
0.11	264.97113	0.6	214.50263
0.12	263.26254	0.61	216.84973
0.13	261.54245	0.62	219.26889
0.14	259.8111	0.63	221.75059
0.15	258.06873	0.64	224.2869
0.16	256.31557	0.65	226.87109
0.17	254.55191	0.66	229.49745
0.18	252.77801	0.67	232.1611
0.19	250.9942	0.68	234.85781
0.2	249.20079	0.69	237.58394
0.21	247.39815	0.7	240.3363
0.22	245.58666	0.71	243.11211
0.23	243.76675	0.72	245.90892
0.24	241.93891	0.73	248.72458
0.25	240.10364	0.74	251.55717
0.26	238.26155	0.75	254.40501
0.27	236.41329	0.76	257.26659
0.28	234.55962	0.77	260.14056
0.29	232.70138	0.78	263.02573
0.3	230.83956	0.79	265.92103
0.31	228.97526	0.8	268.8255
0.32	227.1098	0.81	271.73828
0.33	225.24469	0.82	274.65859
0.34	223.38172	0.83	277.58574
0.35	221.52299	0.84	280.51912
0.36	219.67103	0.85	283.45815
0.37	217.82889	0.86	286.40234
0.38	216.00025	0.87	289.35124
0.39	214.18968	0.88	292.30445
0.4	212.40284		
0.41	210.64692		
0.42	208.93113		
0.43	207.26756		
0.44	205.67237		

0.45	204.16771
0.46	202.78476
0.47	201.56823
0.48	200.58242
0.49	199.91387

Table B9: Liquidus temperature of $LiNO_3$-$NaNO_3$- KNO_3 ternary mixture from thermodynamic model at fixed concentration of $LiNO_3$ at 20%.

X_{BL}	T(°C)	X_{BL}	T(°C)
0.01	255.63303	0.5	175.33016
0.02	254.07985	0.51	176.20045
0.03	252.5146	0.52	177.43933
0.04	250.9373	0.53	178.96635
0.05	249.34798	0.54	180.72284
0.06	247.74667	0.55	182.66578
0.07	246.13339	0.56	184.76295
0.08	244.50817	0.57	186.98971
0.09	242.87103	0.58	189.32677
0.1	241.22198	0.59	191.75884
0.11	239.56106	0.6	194.27354
0.12	237.88828	0.61	196.86076
0.13	236.20366	0.62	199.51214
0.14	234.50723	0.63	202.22069
0.15	232.79903	0.64	204.98052
0.16	231.07908	0.65	207.78664
0.17	229.34742	0.66	210.63478
0.18	227.60412	0.67	213.52127
0.19	225.84922	0.68	216.44295
0.2	224.0828	0.69	219.39708
0.21	222.30496	0.7	222.38125
0.22	220.51581	0.71	225.39339
0.23	218.71549	0.72	228.43167
0.24	216.90417	0.73	231.49448
0.25	215.08207	0.74	234.58041
0.26	213.24945	0.75	237.68822
0.27	211.40662	0.76	240.81682
0.28	209.554	0.77	243.96523
0.29	207.69206	0.78	247.1326
0.3	205.8214		
0.31	203.94276		
0.32	202.05705		
0.33	200.1654		
0.34	198.26923		
0.35	196.37029		
0.36	194.47082		
0.37	192.57364		

0.38	190.68239
0.39	188.8018
0.4	186.93809
0.41	185.09966
0.42	183.29803
0.43	181.54946
0.44	179.87778
0.45	178.31926
0.46	176.93176
0.47	175.81003
0.48	175.09704
0.49	174.93174

Table B10: Liquidus temperature of $LiNO_3$-$NaNO_3$- KNO_3 ternary mixture from thermodynamic model at fixed concentration of $LiNO_3$ at 30%.

X_{BL}	T(°C)	X_{BL}	T(°C)
0.01	227.33064	0.5	148.90297
0.02	225.8623	0.51	150.32284
0.03	224.38132	0.52	152.01908
0.04	222.88756	0.53	153.93826
0.05	221.38083	0.54	156.04127
0.06	219.86096	0.55	158.29868
0.07	218.32776	0.56	160.68781
0.08	216.78103	0.57	163.19086
0.09	215.22056	0.58	165.79359
0.1	213.64611	0.59	168.48448
0.11	212.05747	0.6	171.2541
0.12	210.45437	0.61	174.09462
0.13	208.83657	0.62	176.9995
0.14	207.20379	0.63	179.96324
0.15	205.55576	0.64	182.98117
0.16	203.89219	0.65	186.04933
0.17	202.21276	0.66	189.1643
0.18	200.51718	0.67	192.32316
0.19	198.80513	0.68	195.52336
0.2	197.07627		
0.21	195.33027		
0.22	193.56681		
0.23	191.78554		
0.24	189.98615		
0.25	188.1683		
0.26	186.33169		
0.27	184.47606		
0.28	182.60117		
0.29	180.70684		
0.3	178.79297		

0.31	176.85957
0.32	174.90679
0.33	172.93497
0.34	170.94475
0.35	168.93712
0.36	166.91361
0.37	164.87646
0.38	162.829
0.39	160.77607
0.4	158.72486
0.41	156.68622
0.42	154.67701
0.43	152.72456
0.44	150.87591
0.45	149.21803
0.46	147.91698
0.47	147.21603
0.48	147.22451
0.49	147.83447

Table B11: Liquidus temperature of $LiNO_3$-$NaNO_3$- KNO_3 ternary mixture from thermodynamic model at fixed concentration of $LiNO_3$ at 35%.

X_{BL}	T(°C)	X_{BL}	T(°C)
0.01	205.33802	0.5	128.36337
0.02	203.95609	0.51	130.02728
0.03	202.55964	0.52	131.94085
0.04	201.14829	0.53	134.06201
0.05	199.72168	0.54	136.35846
0.06	198.27942	0.55	138.80509
0.07	196.82108	0.56	141.3821
0.08	195.34623	0.57	144.07369
0.09	193.8544	0.58	146.86709
0.1	192.34511	0.59	149.75186
0.11	190.81784	0.6	152.71938
0.12	189.27206	0.61	155.76248
0.13	187.7072	0.62	158.71938
0.14	186.12265	0.63	161.76248
0.15	184.51779		
0.16	182.89195		
0.17	181.24445		
0.18	179.57455		
0.19	177.88148		
0.2	176.16445		
0.21	174.42261		
0.22	172.65509		
0.23	170.86098		

0.24	169.03933
0.25	167.18917
0.26	165.30949
0.27	163.39928
0.28	161.45751
0.29	159.48318
0.3	157.4753
0.31	155.43298
0.32	153.35547
0.33	151.24223
0.34	149.09305
0.35	146.90829
0.36	144.68912
0.37	142.43806
0.38	140.15978
0.39	137.86257
0.4	135.56101
0.41	133.28149
0.42	131.07381
0.43	129.03508
0.44	127.33236
0.45	126.13557
0.46	125.52146
0.47	125.49878
0.48	126.02083
0.49	127.0042

Table B12: Liquidus temperature of $LiNO_3$-$NaNO_3$-KNO_3 ternary mixture from thermodynamic model at fixed concentration of $LiNO_3$ at 38%.

X_{BL}	T(°C)	X_{BL}	T(°C)
0.01	200.92002	0.5	124.25658
0.02	199.55662	0.51	125.93637
0.03	198.17812	0.52	127.87062
0.04	196.78412	0.53	130.01618
0.05	195.3742	0.54	132.34005
0.06	193.94791	0.55	134.81665
0.07	192.50479	0.56	137.42589
0.08	191.04432	0.57	140.15175
0.09	189.566	0.58	142.98132
0.1	188.06927	0.59	145.90408
0.11	186.55354	0.6	148.78989
0.12	185.01821		
0.13	183.46262		
0.14	181.8861		
0.15	180.28792		
0.16	178.66734		

0.17	177.02356
0.18	175.35574
0.19	173.66301
0.2	171.94443
0.21	170.19904
0.22	168.42583
0.23	166.62374
0.24	164.79165
0.25	162.92844
0.26	161.03291
0.27	159.10386
0.28	157.14008
0.29	155.14034
0.3	153.10348
0.31	151.0284
0.32	148.91418
0.33	146.76014
0.34	144.56603
0.35	142.33232
0.36	140.06056
0.37	137.75416
0.38	135.41964
0.39	133.06905
0.4	130.7249
0.41	128.43087
0.42	126.27511
0.43	124.41078
0.44	122.96247
0.45	121.94729
0.46	121.40055
0.47	121.38489
0.48	121.90271
0.49	122.88784

Communication

Upadhyay, A. and Mittal, M.K. Design of binary and ternary nitrate salt mixtures for energy storage and heat transfer in solar thermal systems. Journal of Solar energy and engineering, Transaction of ASME.

Abhishek_Thesis

ORIGINALITY REPORT

16%	7%	13%	3%
SIMILARITY INDEX	INTERNET SOURCES	PUBLICATIONS	STUDENT PAPERS

PRIMARY SOURCES

1	preserve.lehigh.edu Internet Source	2%
2	Wang, Tao, Divakar Mantha, and Ramana G. Reddy. "Novel high thermal stability LiF–Na2CO3–K2CO3 eutectic ternary system for thermal energy storage applications", Solar Energy Materials and Solar Cells, 2015. Publication	1%
3	Coscia, Kevin, Tucker Elliott, Satish Mohapatra, Alparslan Oztekin, and Sudhakar Neti. "Binary and Ternary Nitrate Solar Heat Transfer Fluids", Journal of Solar Energy Engineering, 2013. Publication	1%
4	Fernández, A. G., A. Rey, I. Lasanta, S. Mato, M. P. Brady, and F. J. Pérez. "Corrosion of alumina-forming austenitic steel in molten nitrate salts by gravimetric analysis and impedance spectroscopy : Corrosion in molten nitrate salts", Werkstoffe und Korrosion, 2014. Publication	1%